Chemico-Biological Interactions 248 (2016) 36–51

Contents lists available at ScienceDirect

Chemico-Biological Interactions

journal homepage: www.elsevier.com/locate/chembioint

Recent conjugation strategies of small organic fluorophores and ligands for cancer-specific bioimaging

Yonghwang Ha, Hyun-Kyung Choi*

Department of Biomedicinal Chemistry, Jungwon University, Munmu-ro 85, Goesan-gun, Chungbuk 367-805, Republic of Korea

ARTICLE INFO

Article history:
Received 3 November 2015
Received in revised form
2 February 2016
Accepted 8 February 2016
Available online 16 February 2016

Keywords:
Near-infrared
Fluorescent diagnosis
Cancer-specific ligands
Cancer-specific receptors
Cancer-specific biomarkers

ABSTRACT

Conjugation between various small fluorophores and specific ligands has become one of the main strategies for bioimaging in disease diagnosis, medicinal chemistry, immunology, and fluorescence-guided surgery, etc. Herein, we present our review of recent studies relating to molecular fluorescent imaging techniques for various cancers in cell-based and animal-based models. Various organic fluorophores, especially near-infrared (NIR) probes, have been employed with specific ligands. Types of ligands used were small molecules, peptides, antibodies, and aptamers; each has specific affinities for cellular receptor proteins, cancer-specific antigens, enzymes, and nucleic acids. This review can aid in the selection of cancer-specific ligands and fluorophores, and may inspire the further development of new conjugation strategies in various cellular and animal models.

© 2016 Elsevier Ireland Ltd. All rights reserved.

Contents

1. Introduction 37
2. Requirements for fluorophore selection and fluorescence application techniques 37
   2.1. Factors impacting fluorophores selection 37
   2.2. Synthesis of fluorophores 37
   2.3. Strategies for selective imaging with high signal to background ratio 37
   2.4. Conjugation techniques between fluorophores and ligands 39
3. Conjugation of specific ligands with fluorophores for diagnostic imaging of various tumors 39
   3.1. Lung cancer 39
   3.2. Breast cancer 42
   3.3. Pancreatic cancer 43
   3.4. Ovarian cancer 44
   3.5. Lymphoma 45
   3.6. Prostate cancer 45
   3.7. Other cancers and cancer-related biological targets 46
   3.8. Perspectives 47
4. Conclusions 48
   Acknowledgements 48
   Transparency document 48
   Abbreviations 48
   References 49

* Corresponding author.
E-mail address: hkchoi45@jwu.ac.kr (H.-K. Choi).

http://dx.doi.org/10.1016/j.cbi.2016.02.006
0009-2797/© 2016 Elsevier Ireland Ltd. All rights reserved.

1. Introduction

A number of biological interactions between ligands and receptors mediate various vital metabolic pathways in the body. Since the interaction between a ligand and a biomarker or cellular receptor is highly specific, various biotechnologies have adopted the ligand-receptor affinity, including fluorescent labeling applications; enzyme-linked immunosorbent assay (ELISA), immunoblotting, diagnosis kits, and fluorescence-based cancer imaging.

In particular, many receptors specific to cancer cells or target molecules are present on cell surfaces and thus have been extensively employed for disease diagnosis and treatment [1]. The early diagnosis of cancer helps to ensure better prognosis of treatments. Various tools have been employed for cancer diagnosis, including nuclear magnetic resonance (NMR), computed tomography (CT), positron emission tomography (PET), and single-photon emission computerized tomography (SPECT), and fluorescent imaging [2,3]. Among them, fluorescent imaging shows excellent potential as a diagnostic tool for *in vitro* and *in vivo* cellular monitoring because it is highly sensitive and selective and is inexpensive to handle. Specifically, the use of fluorophores targeted to cancer-specific ligands has been adopted for cancer diagnosis.

Generally, there are three main strategies for treating cancer, surgery, radiotherapy, and chemotherapy. Among them, surgery is the most widely used cancer treatments. However, surgery has serious limitations in improving the survival rate of patients because the border between cancer and normal cells cannot be clearly discriminated by the naked eye. This challenge could result in the removal of healthy cells or residual cancerous tissue remaining. Recently, for improved outcomes, fluorescence-guided surgery has been widely employed in the treatment of cancer [4–6]. One of the greatest challenges in developing effective treatments for cancer is their obscure boundary which is from tissue invasion and metastasis. Differentiation of clear border of cancer tissue from normal tissue is necessary to prepare the promising cancer therapeutics [7,8].

There have been numerous reviews focused on fluorescence-based cancer imaging [1,3,9]. Some mention various design schemes allowing for the use of fluorescent probes in medical diagnostic imaging via photoinduced electron transfer (PeT), Förster resonance energy transfer (FRET), activation-quenching based fluorescent OFF-ON system, or fluorescent lifetime imaging (FLIM) strategies, which can be adopted for the development of fluorophores having high signal to background ratio [3,9]. A separate review outlines combinatorial strategies for the development of fluorescent probes through target or diversity-oriented fluorescent libraries screening, powerful methods capable of identifying high potential fluorophores or ligands [10]. In addition, other reviews describe various synthesis and conjugation strategies for fluorophores and biomarker-specific ligands [11–14]. Gonçalves reviewed various types of organic fluorophores, with potential utility in the labeling of biomolecules. She introduced various research efforts for *de novo* construction of fluorophores according to emission wavelength; less than 500 nm, more than 500 nm, and NIR region [12].

In this review, we summarize various factors for the designing conjugated molecules with cancer-specific fluorophores, specifically focusing on *i*) cancer-specific biomarkers, *ii*) biomarker specific ligands, *iii*) fluorophores, and *iv*) conjugation of fluorophores and biomarkers from recent published literature (Fig. 1). The focus of this review is *organic* or *organometallic* fluorophore-conjugated systems (mainly organic molecules), not inorganic fluorophores, or quantum dots system.

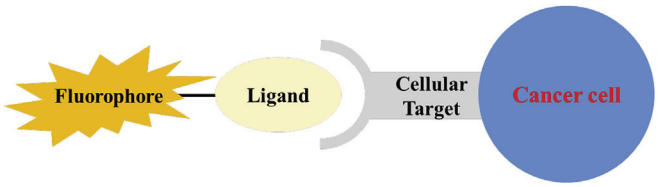

Fig. 1. Scheme for fluorescent imaging via conjugation between fluorophore and a cellular target-specific ligand.

2. Requirements for fluorophore selection and fluorescence application techniques

2.1. Factors impacting fluorophores selection

A number of fluorochromes have been developed and applied to various topics including: *i*) chemical sensing, *ii*) cellular imaging, *iii*) protein labeling, *iv*) fluorescence analysis, and *v*) medicinal chemistry (Fig. 2). When using fluorophores in biological systems, some key factors should be considered prior to their selection: *i*) wavelengths of excitation and emission, *ii*) emission intensity, *iii*) solubility, and *iv*) stability. For the selection of fluorophores, consideration of excitation wavelength and emission wavelength is very important [15]. Although there are a variety of fluorophores display various emission wavelengths, from violet to red or NIR, a short wavelength (300 nm ~ 500 nm) can be disturbed by cytoplasmic materials and penetration depth is not deep, meaning the influencing space is small. However, longer wavelength light, red or NIR, of fluorophores makes low interference with biological materials and long depth penetration, which helps clear noninvasive cellular tumor imaging with high signal to background ratio [3]. Strong emission signal is crucial for obtaining high signal to background ratio. Intensity of emission depends on quantum yield under various solvents. Aqueous condition must be considered for selection of fluorophores because many organic fluorophores did not emit fluorescence in aqueous solution from the self-quenching by π-π stacking of resonance structure. For water solubility, sulfur oxide group can be inserted without disturbing photophysical properties of fluorophores [15].

2.2. Synthesis of fluorophores

Most fluorophores employed for bioimaging are usually commercial because they may be easy and convenient for handling. However, for the best use of fluorophores, *de novo* synthesis should be employed. The following articles are good sources of information about methods for the *de novo* synthesis of five main fluorophores; BODIPY [16], Rhodamine [17,18], Fluorescein [19–21], cyanine NIR fluorophores [22,23].

2.3. Strategies for selective imaging with high signal to background ratio

For the design of OFF-ON fluorescence probing systems, many strategies are employed especially, PeT, FRET, and FLIM, etc. [24]. In particular, PeT is extensively used for the design of OFF-ON fluorescence detection. When one electron is transferred to the empty ground state from a nearby quenching ligand after excitation of a fluorophore, fluorescence is quenched (reductive PeT). However, after removing the quencher from the fluorophore-quencher conjugated molecules by lysosomes after uptake into cellular systems, selective high fluorescence can be generated [3]. FRET is usually employed for the determination of three-dimensional (3D) structure of a protein, whose properties are

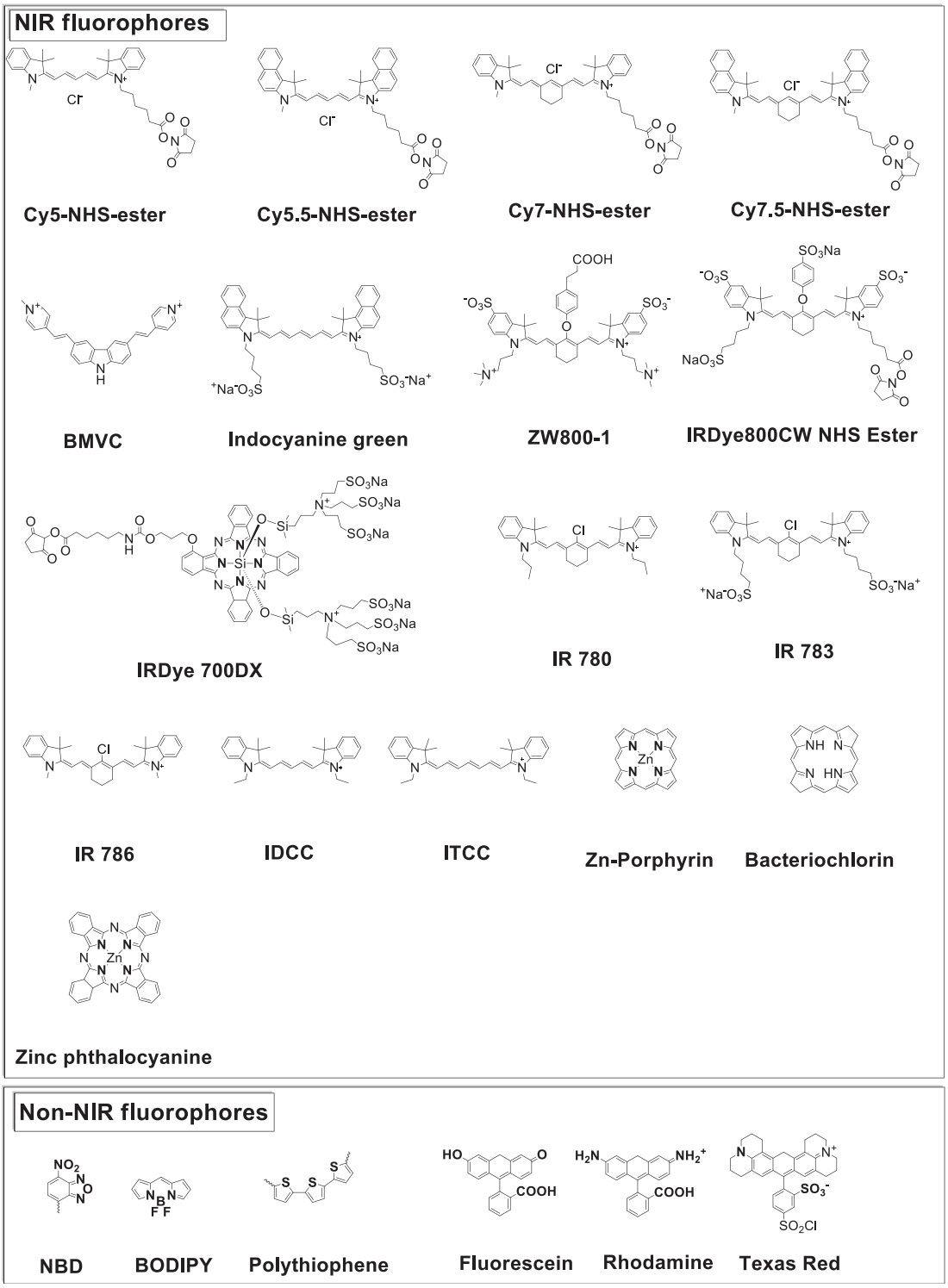

Fig. 2. Various fluorescent molecules applied for cancer imaging.

related to distance between two different fluorophores. Emission intensity decreases as the fluorophore's distance increases ($1/r^6$). For cellular imaging, two fluorophores can be conjugated with two proteins which are capable of dimerization. According to the dimerization status of these proteins, two different fluorescent signals can be obtained, signals from monomer or dimer, which can provide important information related to distance and dimerization status of two proteins [25]. Relative to fluorescence imaging, FLIM shows different properties. FLIM signals depend on the time of fluorescence decay which is induced by micro-environmental changes, such as the composition and the function of tissue, not by concentration of fluorophores, excitation intensity, and attenuation due to tissue absorption and scattering [26].

ITM Exhibit 1023, Page 3 of 16

2.4. Conjugation techniques between fluorophores and ligands

For conjugation between fluorophores and biological materials, it will be useful to consider several connection strategies. Valuable information about fluorescent labeling techniques relating to biological molecules (including proteins) are found in the literature [11,14]. In particular, Hermanson reviews a number of studies about conjugation properties between various functional groups [11]. Conjugation strategies were described relating to main functional groups including amines, carboxylic acids, hydroxyls, and thiols (Figs. 3–6).

Without specific activation, an amine group can be connected with various activated functional groups; isothiocyanate, isocyanate, acyl azide, *N*-hydroxysuccinimide (NHS), sulfonyl chloride, aldehyde, epoxide, carbonate, fluorobenzene, and succinic anhydride (Fig. 3) [11,14]. In particular, isothiocyanate and NHS are widely employed as functional groups for targeting an amine group, e.g., Fluorescein isothiocyanate (FITC) [27], fluorophore-NHS-esters [28]. Aldehyde groups can also react with a primary amine to generate the Schiff base, which is transferred to a secondary amine group after reduction. Interestingly, succinic anhydride can change the functional group of a molecule from primary amine to carboxylic acid, which may be helpful for more elaborate targeting situations.

For carboxylate group, various activation groups are strongly required because of its stable resonance structure (Fig. 4) [11,14]. Carbodiimide compounds, such as 1-ethyl-3-(3-dimethylaminopropyl)carbodiimide (EDC), *N*,*N*′-Diisopropylcarbodiimide (DIC), and *N*,*N*′-Dicyclohexylcarbodiimide (DCC) are widely used as activation compounds. In addition, carbonyl diimidazole (CDI), sulfo-NHS, and thionyl chloride can be useful for activation of the carboxylate group. After activation, various functional groups can be coupled with the carboxylate group, such as, primary amines, hydroxyls, and thiols to generate imide, ester, and thio ester compounds. Interestingly, diazoacetate can be connected with the carboxylic acid without activation.

Hydroxyl groups also should be activated for coupling with various functional groups (Fig. 5) [11,14]. Similarly with the carboxylate group, EDC, DIC, DCC, and CDI, can be employed to activate the hydroxyl group. Additionally, tosyl chloride and *N*,*N*′-disuccinimidyl carbonate (DSC) are useful activators for hydroxyl groups. After activation, various nucleophiles can be conjugated to generate secondary amine, ether, sulfide, urethane, and imide compounds. Isocyanate can be directly linked to the hydroxyl group to induce a urethane moiety.

Thiol groups can be useful as docking sites for various fluorophores in specific enzyme containing cysteine residues (Fig. 6) [11,14]. Maleimide derivatives, iodoacetyl compounds, aziridines, acryloyl derivatives, fluorobenzenes, and disulfide compounds are adopted to specific connection without specific activation (Fig. 6). In particular, a disulfide compound can be exchanged with one thiol group to generate an R-R′ combined molecule.

3. Conjugation of specific ligands with fluorophores for diagnostic imaging of various tumors

In this chapter, we describe the conjugation strategies of various organic fluorophores and biomarker-specific ligands presented in the literature for imaging of various cancers including lung cancer, breast cancer, pancreatic cancer, ovarian cancer, lymphoma, prostate cancer, other cancers, and cancer-related biological targets.

3.1. Lung cancer

Various biomarkers have been adopted for targeting and cellular imaging of lung cancers including aminophospholipids exposed, platelet/endothelial cell adhesion molecule 1 (PECAM 1) in tumor vasculature, and αvβ3 integrin, etc. (Table 1). As shown in Table 1, while one specific peptide ligand was applied only for imaging of H460 lung tumor cells, other ligands showed broad-spectrum

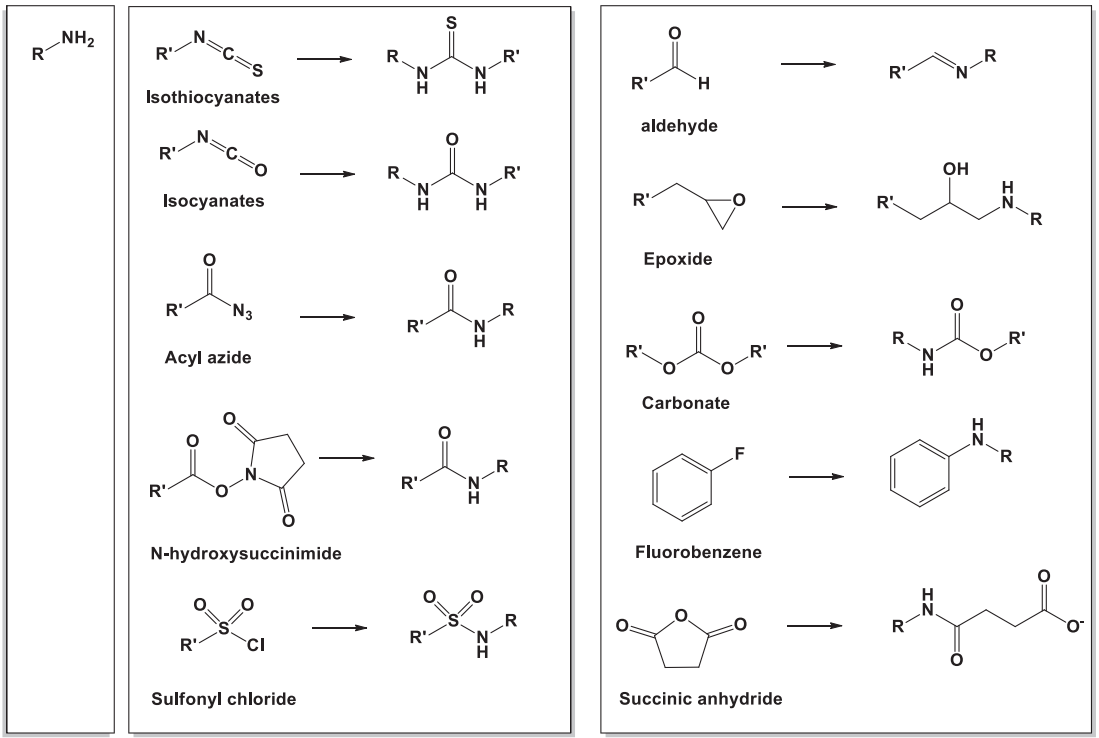

Fig. 3. Conjugation strategies for an amine group with various functional groups [11].

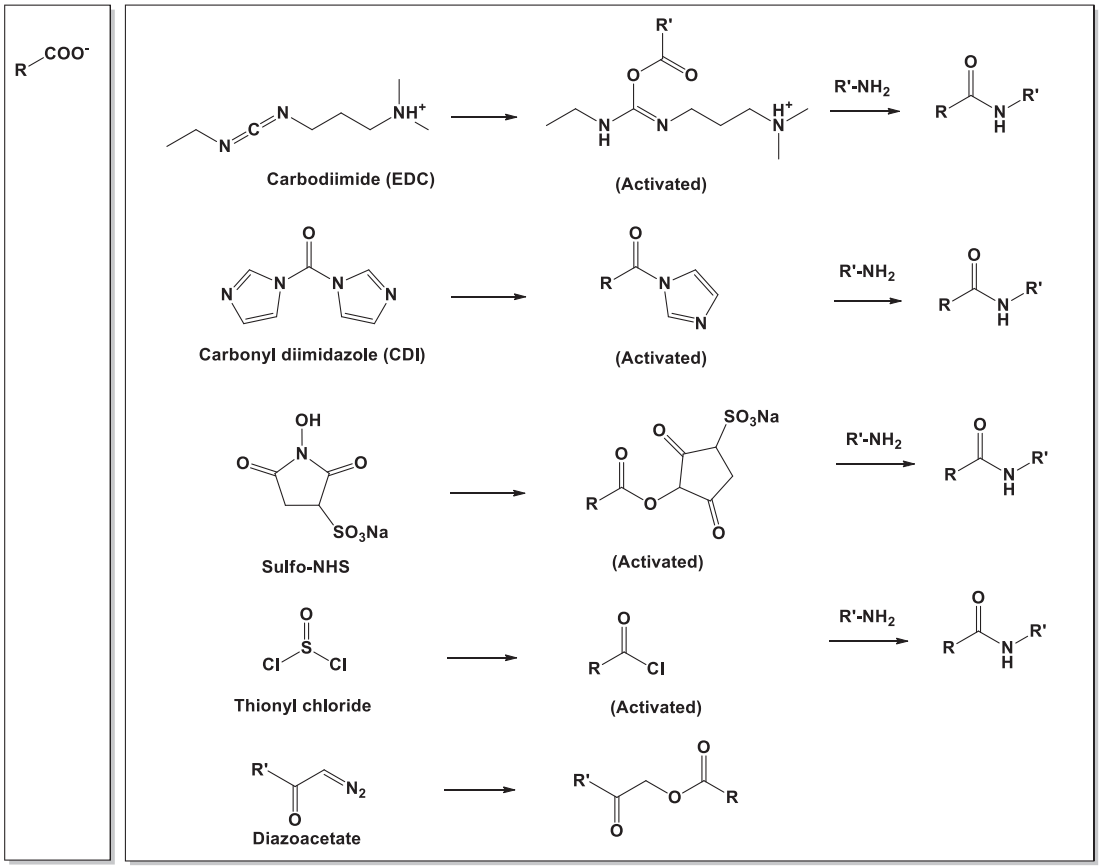

Fig. 4. Conjugation strategies for a carboxylate with various functional groups [11].

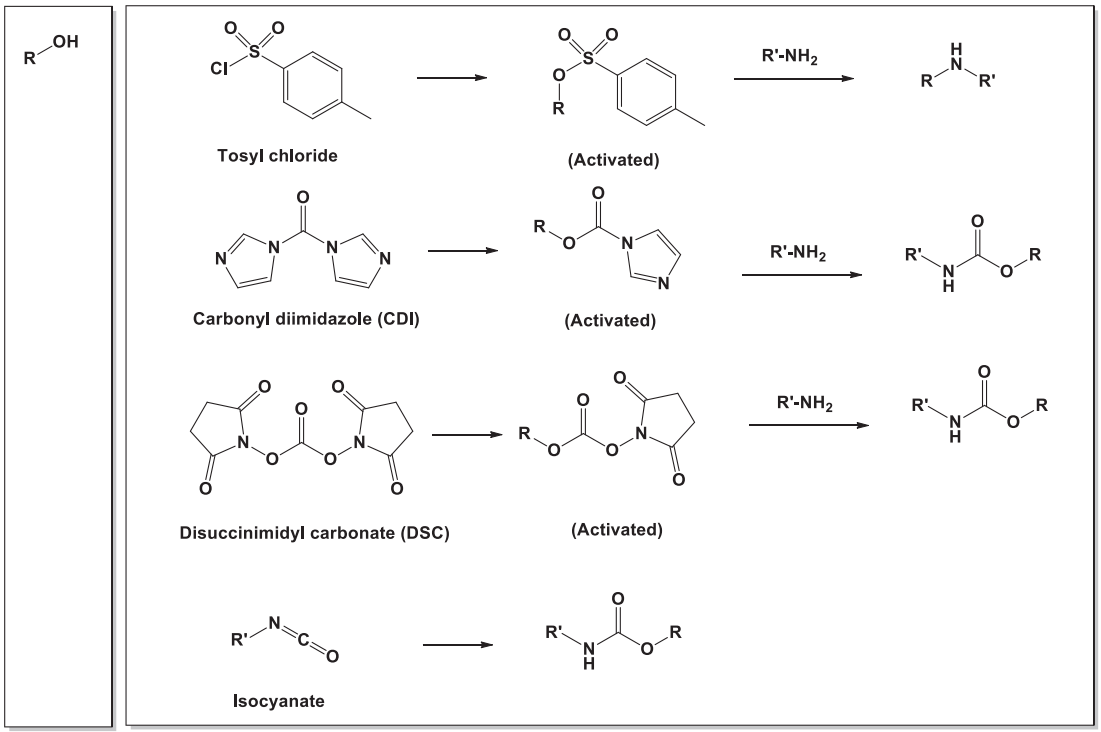

Fig. 5. Conjugation strategies for a hydroxyl group with various functional groups [11].

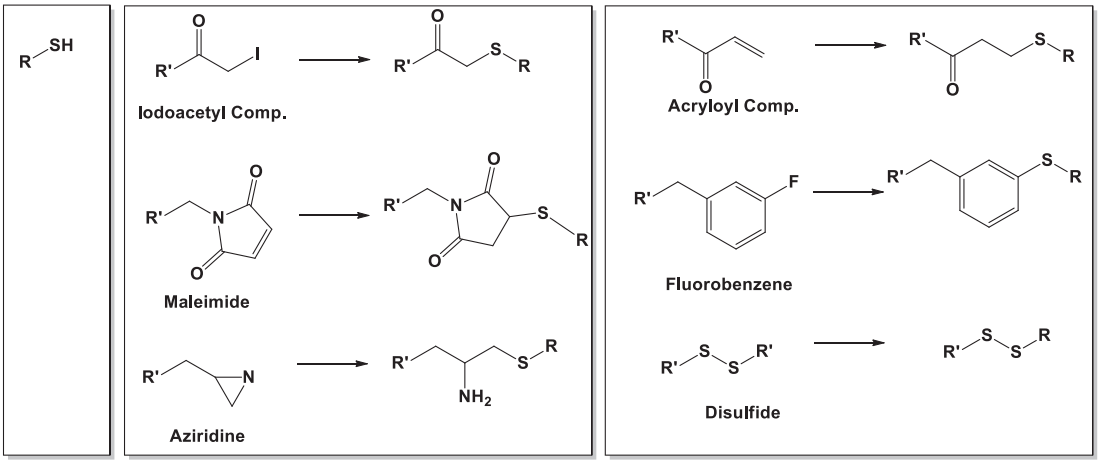

Fig. 6. Conjugation strategies for a thiol group with various functional groups [11].

specificity. Proteins which have binding affinity to cancer-specific biomarkers were used for conjugation with fluorophores including annexin, endostatin, avidin, neomannosyl human serum albumin, and antibodies. While certain types of ligands are composed of peptides (cyclic RGD and CSNIDARAC peptide), the others were small molecules or drugs (folate and cisplatin). For the selection of fluorophores, commercial NIR dyes were usually adopted; Cy5, Cy5.5, Rhodamine X, Fluorescein, 3,6-bis(1-methyl-4-vinylpyridinium) carbazole diiodide (BMVC), and indocyanine green (ICG), while ZW800-1, and polythiophene were constructed with *de novo* synthetic methods.

More specifically, Petrovsky et al. used fluorescence-imaging techniques for gliosarcoma and lung carcinoma [28]. Specifically, they were able to label the apoptotic process using an NIR probe based on Cy5.5 conjugated with annexin, a protein having a specific affinity for aminophospholipids externalized during apoptosis.

The generation of blood vessels is critical during tumor progression and many studies have been focused on developing inhibitors of endostatin activity. Camphausen and colleges used a Cy5.5-based NIR probe attached to endostatin, a molecule which is involved in angiogenesis during tumor progression [29]. This group utilized endostatin for tumor imaging. They found endostatin-Cy5.5 homed at tumor vasculature and interacted with PECAM 1 expression.

It has been known that cRGD has binding affinity to the αvβ3 integrin protein found on the cellular surface. Coll and colleagues employed a cyclic RGD peptide connected with Cy5 via cyclic decapeptide linker, called RAFT [30]. They tried to connect four cRGD ligands with a Cy 5 NIR dye covalently to view lung tumor cells. This approach increased targeting specificity. Also, Tseng et al. attempted to trace guanine-rich oligonucleotides (GROs), a therapeutic target for tumors [31]. They used 3,6-bis(1-methyl-4-vinylpyridinium) carbazole diiodide (BMVC) or Cy5 as fluorophores and covalently linked these to two types of GROs, parallel and non-parallel G4 structures. They were able to monitor GROs' cellular uptake and movement in CL1-0 lung adenocarcinoma cells using fluorescent imaging via FRET. Also, Frangioni and research fellows presented an interesting report about an indotricarbocyanine (ITCC)-based NIR probe, ZW800-1 [35]. This probe, having innate zwitterionic property, was connected with cRGD peptide, fibrinogen or antibodies for use in *in vitro, in vitro* tumor imaging. For selective imaging of lung cancer, they adopted cRGD

Table 1
Conjugation of fluorophores and biomarker-specific ligands for bioimaging of lung cancer.

Fluorophore	Ligand	Biomarker	EX/EM[a] (nm/nm)	Disease	Ref
Cy5.5	Annexin	Aminophospholipids externalized	635/710	Tumor apoptosis in Gliosarcoma and lung carcinoma	[28]
Cy5.5	Endostatin	PECAM 1 in tumor vasculature	675/694	Lewis lung carcinoma tumor	[29]
Cy5	cRGD	αvβ3 integrin	633/	human non small-cell lung carcinoma, human ovarian cancer	[30]
Cy5	GRO	(to monitor intracellular movement of GROs)	633/660–750	Lung cancer cell	[31]
BMVC	GRO	(to monitor intracellular movement of GROs)	633/660–750	Lung cancer cell	[31]
Rhodamine, QSY7	Avidin	D-galactose receptor	530–585/605–680	metastatic lung tumors	[32]
BODIPY	Ab against HER2	HER 2	480/500–800	Lung Tumor	[33]
Fluorescein	CSNIDARAC peptide	Surface receptor (Not specified)	–	H460 lung tumor cells	[34]
ZW800-1	cRGD	integrin αvβ3	/800	Liver, Lung tumor	[35]
Polythiophene	cisplatin	(to monitor intracellular movement of cisplatin)	455/600	Adenocarcinomic human alveolar basal epithelial cells (A549 cell)	[36]
Fluorescein	folate	Folate receptor α	465–490/520–530	lung adenocarcinomas (clinical study)	[27]
ICG	Neomannosyl human serum albumin	Mannose receptors on macrophages	690–790/800	Sentinel Lymph Node in lung cancer (clinical study)	[37]
ICG	Serum albumin (non-covalently binding to ICG)	(Not specified)	690–790/800	Clinical stage I non-small-cell lung cancer (clinical study)	[38]

[a] EX: Excitation wavelength, EM: Emission wavelength.

ITM Exhibit 1023, Page 6 of 16

which is specific to the integrin protein αvβ3. They reported that this probe showed improvements over the commercial probes IRDye800-CW and Cy5.5.

Kobayashi and colleges reported on the fluorescent detection of *in vivo* lung cancer metastases [32]. They employed a fluorophore-quencher modality for more specific detection, which means specifically turn-ON when inside tumors and not outside or when inside normal cells. They used an avidin protein which can bind to the D-galactose receptor to induce endocytosis and degradation in lysosomes. Disconnection of fluorophores from quenchers induced strong turn-ON emission selectively in the lung tumor. In addition, Kobayashi and his colleges also designed a targeted 'activatable' fluorescent imaging probe [33]. They conjugated a BODIPY fluorophore to an antibody, specific to human epidermal growth factor receptor type (HER) 2 protein. They designed BODIPY to turn-ON at the acidic pH found in lysosomes after internalization by the tumor cells. Therefore, they were able to probe lung cancer cells and tissues with high target-background signal.

Lee and colleges reported an imaging probe with targeted delivery ability using liposomal doxorubicin to lung tumor [34]. They employed a screening method of a phage-displayed peptide library. A CSNIDARAC peptide was highly effective to selective binding to H460 lung tumor cells. When doxorubicin was joined with the Fluorescein probe as liposomal type, it was successfully targeted to the lung cancer.

Wang and colleges reported about an amphiphilic fluorophore conjugated with cisplatin which is a platinum-connected anticancer drug [36]. At first, they showed nontoxicity of polythiophene fluorophore, and tested the fluorophore for imaging lung tumor cells. This conjugated fluorophore-drug showed good potentiality of pharmacokinetics as an anticancer drug.

Kim and colleagues performed fluorescence imaging on lung cancer using indocyanine green (ICG) NIR fluorophore linked to neomannosyl human serum albumin (MSA) in rat model [37]. Relative to human serum albumin (HSA), MSA can easily be penetrated into interstitial tissues to lymphatic capillaries, but not to blood capillaries, thus providing more specific binding to the mannose receptor on macrophages allowing for better tumor imaging. Additionally, LD_{50} of ICG has been known as of 50–80 mg/kg for animals, and it can be excreted rapidly almost in the bile [39].

As a clinical trial for lung cancer treatment, fluorescence imaging can be helpful for tumor surgery. Singhal and coworker reported intraoperative molecular imaging on lung adenocarcinomas from patients during pulmonary resection using fluorescein probe [27]. They connected the probe with a folate, folate-FITC, capable of binding specifically to the folate receptor α in the lung adenocarcinoma. For toxicity information, they reported that there were not any severe toxicity relating to injection of folate-FITC, although one patient showed mild hives and another displayed some irritation at the injection site among a total of 50 patients, between ages 25 and 85 years (mean: 67 years). Four hours before surgery, the folate-FITC conjugate (0.1 mg/kg) was administered intravenously. During surgery, tumor fluorescence images were monitored *in situ* and *ex vivo*. Using this connected probe, they were able to successfully remove the tumor tissue during surgery.

Yamashita group utilized ICG as a fluorophore for imaging non-small-cell lung cancers which were at clinical stage I [38]. Interestingly, no ligand was conjugated in targeting specific cellular materials They administered 2 mL of ICG (5 mg/ml) around the tumor and checked sentinel nodes after 10 min using video-assisted thoracoscopic imaging apparatus. They were able to identify sentinel nodes by NIR fluorescence imaging methods which were consistent well with the results from segmentectomy or lobectomy methods. The overall accuracy rate was 80.7%.

3.2. Breast cancer

Table 2 shows that proteins, small peptides, small organic molecules, and drugs have been used in the bioimaging of breast cancer. Protein ligands include epithermal growth factor (EGF), transferrin, and antibodies. Peptide ligands were specific enough for targeting proteins in breast cancer. In addition, small drugs were employed for imaging of specific enzymes for pharmacokinetic purposes.

Overexpression of EGF receptor (EGFR) has been well known in various cancers of the brain, breast, colon, head, neck, lung, ovary, and pancreas and as such the EGF ligand has relatively broad-spectrum specificity for various cancers [40,41]. Li et al. reported an EGF-Cy5.5 conjugation optical probe [40]. They found that the EGF-Cy5.5 compound was well internalized in MDA-MB-468 breast cancer cells and mouse tissue to allow for strong fluorescent imaging of cancers.

Some experimental evidence indicates an interaction between interleukin (IL) 11 and interleukin 11 receptor alpha-chain (IL-11Rα) may be involved in thee metastasis of human breast cancer to the bone [42,43]. Wang et al. attempted to connect a cyclic peptide, c(CGRRAGGSC), to an IR-783-derived NIR fluorophore [44]. This cyclic peptide ligand has been known as a binding ligand for IL-11Rα. They successfully imaged breast cancer cells in mice models of breast cancer.

It is known that *glu*cose *t*ransporter (Glut) 5 tends to be overexpressed in tumors relative to normal tissue. Similarly, Gambhir and coworkers employed 7-nitro-1,2,3-benzadiazole (NBD) and Cy5.5 fluorophores for imaging breast cancer cells [45]. Interestingly, they used fructose, which can interact with a Glut5 as the ligand. The conjugated compounds fructose-Cy5.5 or fructose-NBD, showed internalization and emission of fluorescence in breast cancer cells. Also, Ramanujam and her colleges reported delivery-

Table 2
Conjugation of fluorophores and biomarker-specific ligands for bioimaging of breast cancer.

Fluorophore	Ligand	Target	EX/EM (nm/nm)	Disease	Ref
Cy5.5	EGF	EGFR	660/710	Breast Cancer Xenografts	[40]
IR-783	c(CGRRAGGSC)	IL-11RR	785/830	Human breast cancer	[44]
Cy5.5	Fructose	Glut5	640/700	Breast cancer	[45]
NBD	Fructose	Glut5	450–490/515–565	Breast cancer	[45]
Fluorescein	trastuzumab	HER2	493/515	Breast cancer	[47]
NBD	glucose	Glut	470/520–620	Murine Breast Cancer	[46]
Cy5	CLKADKAKC (CK3)	NRP-1	–	Breast cancer	[48]
Cy5, Fluorescein	LXL-1	Specific sites in DNA	–	Metastatic Breast Cancer Cell	[49]
AlexaFluor700, AlexaFluor750	Transferrin	Transferrin receptor	695/690–1020	Breast Cancer Cells	[25]
ZW800-1	antibody to the c-erbB-2 oncoprotein	c-erbB-2 oncoprotein	800	Breast cancer cell	[35]
Cy5.5	MT1-AF7p (HWKHLHNTKTFL)	MT1-MMP	675/695	Human breast carcinoma cell	[50]
Texas Red	AZD2281	PARP 1	560/630	Human breast adenocarcinoma	[51]
Indigo Carmine dye + ICG	(no specific ligand)	(not specified)	760/380–1200	Early stage breast cancer (Clinical study)	[52]

corrected imaging of breast cancer cells using fluorescently-labeled glucose targeting Glut on the surface of cancer cells [46]. They conjugated a NBD fluorophore to glucose, and used this to image breast cancer cells. They demonstrated the interaction of vascular oxygenation and differentiating metabolic phenotypes *in vivo*.

In addition, DaCosta and colleagues applied trastuzumab, a dual labeled antibody conjugated to the fluorophore and quencher, Fluorescein and black hole quencher 3 (BHQ3), respectively [47]. Trastuzumab has specific binding affinity to the HER 2 receptor on the surface of breast tumors. They demonstrated the feasibility of detecting tumor margins which in turn can effectively guide surgeries using this conjugated probe.

Zeng and coworkers reported their strategy of conjugating a small peptide to an NIR probe [48]. They screened phage libraries to find peptides which bind to breast cancer cells with high affinity, and sequenced these peptides. From this work they suggested that CLKADKAKC (CK3), which contains a cryptic C-end rule motif, binds to neuropilin-1, a multifunctional membrane receptor related with angiogenesis. They demonstrated that the peptide had excellent probing ability in breast cancer cells and mouse tissues with the conjugated NIR-CK3 molecule.

Yang and coworkers employed the cell-based systematic evolution of ligands by exponential enrichment (SELEX) method to search an appropriate DNA-sequenced aptamer which exhibits selective probing ability for the breast cancer cell line, MDA-MB-231, which are derived from a metastatic site-pleural effusion [49]. They showed that a specific aptamer ligand, GAATTCAGTCGGACAGCGAAGTAGTTTTCCTTCTAACCTAAGAACCCGCGGCAGTTTAATGTAGATGGACGAATACGTCTCCC, which is named as LXL-1, showed good binding affinity. They conjugated this aptamer with a Cy5 NIR dye. This conjugated aptamer probe exhibited good imaging potential on metastatic breast cancer cell lines, not non-metastatic cells, with high selectivity.

Also, Barroso et al. describe a method which can discriminate the bound and internalized transferrin from free and soluble transferrin using the NIR fluorescence lifetime FRET technique. Using AlexaFluor700 and AlexaFluor750 as fluorophores, each conjugated with transferrin, they were able to detect bound and internalized forms of transferrin in breast cancer cells and tumors using animal models.

Chen and fellows screened Ph.D.-12™ phage display peptide libraries to find appropriate ligands for targeting membrane type-1 matrix metalloproteinase (MT1-MMP) which has been known to inhibit pericellular proteolysis of extracellular matrix macromolecules to induce tumor development, angiogenesis, and metastasis [50]. They found a peptide, HWKHLHNTKTFL, which they named MT1-AF7p, displayed excellent binding affinity. This peptide ligand was conjugated with Cy5.5 NIR dye and employed to image MT1-MMP-expressing tumors. This approach, displayed good detection ability.

Specific drugs or inhibitors can be a good selective ligand for a specific enzyme when sensing tumors. The research group led by Weissleder attempted to probe an enzyme, poly(ADP-ribose) polymerase (PARP) 1 which plays an important role in sensing DNA damage and initiating the base excision repair pathway [51]. They synthesized a drug, AZD2281 inhibitor, which is known to be a good binding ligand for PARP 1, and conjugated this with Texas Red fluorophore, a rhodamine-based fluorophore. Successful fluorescent NIR imaging was demonstrated in MDA-MB436 breast cancer cells.

For a clinical trial, there was a study on utilizing ICG as fluorophore to image sentinel lymph nodes (SLNs) relating to early breast cancer [52]. Interestingly, without any specific ligand, Toh group was able to detect SNLs as well as lymphatic vessel with the assistance of HyperEye Medical System (HEMS). A mixture (4 mL) of Indigo Carmine dye (15 mg) and ICG (1.75 mg) was administered into the subareolar region of the breast. After 5 min for dilatation to the breast lymphatics, ICG fluorescence illumination was attempted. It was remarkable that detection rate for SNLs was 100%, for all patients and the sensitivity for metastatic involvement was 93.8%, which was verified by histopathology.

3.3. Pancreatic cancer

Table 3 depicts strategies for conjugating fluorophores and various ligands which are specific target molecules in pancreatic cancer cells or tissues. In this case, small peptides such as cytate and cybesin or small organic molecules, e.g., olaparib, were utilized as ligands, and these ligands are conjugated with various commercial NIR fluorophores.

More specifically, Dorshow's group developed a dye-peptide conjugate platform for fluorescent imaging of pancreatic acinar carcinoma [53]. They conjugated a cypate dye, an indocyanine-based NIR fluorophore, with small peptides, octreotate and bombesin derivatives, to prepare the cytate and cybesin conjugation probes, respectively. While octreotate derivative was aimed to target to a somatostatin receptor, bombesin derivative was targeted to a bombesin receptor. The conjugated probes were treated and evaluated *in vivo* in well-characterized rat tumor lines expressing somatostatin and bombesin receptors. They demonstrated that these conjugated molecules can be successful for contrast viewing of pancreatic acinar carcinoma.

Additionally, Weissleder and co-researchers reported a bioorthogonally-developed companion imaging drug (CID) [54]. One biorthogonal method was fluorescence imaging composed of the BODIPY fluorophore and olaparib. Olaparib is an inhibitor for PARP, meaning that it has good selective affinity for PARP. In this study, they showed CID, BODIPY-Olaparib, has good imaging

Table 3
Conjugation of fluorophores and biomarker-specific ligands for bioimaging of pancreatic cancer.

Fluorophore	Ligand	Target	EX/EM (nm/nm)	Disease	Ref
Indocyanine	Octreotate derivative	Somatostatin receptor	780/830	Pancreatic Acinar Carcinomas	[53]
Indocyanine	Bombesin derivative	Bombesin receptor	780/830	Exocrine rat pancreatic acinar carcinoma	[53]
BODIPY	Olaparib	PARP	473/490–540	Ovarian and pancreatic cell	[54]
Cy7.0	AGFSLPAGC	Cathepsin E	–	pancreatic ductal adenocarcinoma, pancreatic intraepithelial neoplasias	[55]
Cy5.5	C-CPE	Claudin-4	665/694	Pancreatic cancer	[56]
IR800CW	PEGO-Cys(*S*-[2,3-bis(palmitoyl)oxy-(*R*)-propyl])-Gly-DSer-PEGO-NH_2	TLR 2	710–760/810–875	Pancreatic cancer	[57]
Cyanine (asymmetrically modified)	AREPPTRTFYWG	uMUC-1 tumor antigen	790/840	Human pancreatic adenocarcinoma, CAPAN-2	[58]

potential for PARP cellular distribution in pancreatic tumor cells, verified with PET-CT imaging bioorthogonally.

It has been known that cathepsin E is specifically overexpressed in pancreatic ductal adenocarcinoma and pancreatic intraepithelial neoplasias. Cheng and researchers achieved the development of conjugated molecules between Cy7.0 and a AGFSLPAGC peptide ligand [55]. The fluorescent probe displayed increased the fluorescent signal ratio of pancreatic tumor to normal pancreatic cells with progression of pathological grades in heterotropically-implanted tumors generated from CTSE-overexpressing PANC-1 cells in nude mice and in 7,12-dimethyl-1,2-benzanthracene (DMBA)-induced rats. Also, for the fluorescent imaging of pancreatic cancer, Gress and colleagues developed a claudin-4-targeted optical imaging technique [56]. Interestingly, by employing the C-terminal partial fragment of *Clostridium perfringens* enterotoxin (C-CPE) as a ligand, they could detect claudin-4 with high selectivity but non-toxicity. Claudin-4 is an integral component of tight junctions and highly expressed in various gastrointestinal tumors including pancreatic cancer [56]. By conjugation of this peptide ligand with Cy5.5 NIR probe, they demonstrated the potential for quality cellular imaging in claudin-4 positive CAPAN1 cells.

Vagner and colleagues developed a fluorescent targeting strategy for the Toll-like receptor (TLR) 2 in pancreatic cancer [57]. They designed, synthesized, and characterized a novel synthetic TLR 2 agonist—PEGO-Cys(*S*-[2,3-bis(palmitoyl)oxy-(*R*)-propyl])-Gly-DSer-PEGO-NH_2 (PEGO: an acetylated 20-atom ethylene glycol oligomer). They conjugated the ligand with IR800DyeCW and attempted to image a pancreatic cancer. They obtained good fluorescent image with low background signal via the affinity of TLR 2 with the agonist ligand.

The Moore group used a water-soluble NIR dye for the molecular imaging of human pancreatic adenocarcinoma [58]. They prepared an asymmetric NIR fluorophore using a *de novo* synthetic method and conjugated this fluorophore with a specific peptide ligand, AREPPTRTFYWG, This ligand was synthesized to target mucin-1 tumor antigen (uMUC-1), which is an early biomarker for the tumorigenesis of various malignancies [59–61]. They demonstrated that this conjugated NIR fluorophore displayed excellent probing potential *in vitro* and *in vivo* in human pancreatic adenocarcinoma CAPAN-2.

3.4. Ovarian cancer

Table 4 describes conjugation methods between fluorophores and various ligands which are specific ovarian cancer-related targets. Folate showed broad spectrum utility for cancer imaging, and was adopted here as well as in lung adenocarcinoma. Although almost all fluorophores were commercially available, Si-rhodamine was synthesized using the *de novo* method. Two kinds of human serum albumin were also employed for connection or delivery of fluorophores as broad-spectrum ligands, which are the same as lung cancer.

In detail, a folate molecule was connected with an asymmetrical cyanine NIR dye which was prepared using a *de novo* method. It has been known that the folate receptor is highly expressed in ovarian cancer cells [72,73]. The Weissleder group developed an ovarian cancer cell imaging technology [62]. They used a folate molecule as a ligand targeted for the folate receptor in ovarian cancer cells and linked this with a cyanine NIR fluorophore. Successful imaging was displayed in ovarian cancer cells and animal tissues using this conjugated molecule.

Kobayashi and coworkers developed a target-specific molecular imaging strategy using the dequenching method [63]. When three Rhodamine X-based fluorophores were conjugated with an avidin tetramer protein, fluorescence was self-quenched. However, when the conjugated form was internalized by the cell and dissociated in lysosomes of the cancer cells, the liberated fluorophores displayed turn-ON fluorescence, which expressed excellent selective tumor imaging to background signal. In addition, Kobayashi et al. employed another technique for probing blood contamination, bloody ascites or hemorrhages during surgery, which can be useful during clinical application of fluorescence imaging [68]. They obtained cellular imaging from fluorescent lifetime information. They used a probe of galactosyl serum albumin (GSA) conjugated with Rhodamine green, which targets the D-galactose receptor. Although the quality of the fluorescence imaging was affected by the concentration of conjugated fluorophores or the addition of blood, FLIM displayed constant signal regardless of these disturbances. FLIM was able to clearly detect changes in the microenvironment, especially tumor lesions under hemorrhagic peritonitis. Also, Kobayashi and co-workers introduced multicolor *in vivo* imaging techniques using bacteriochlorin-based NIR fluorophores, named as NMP4, and NMP5 [69]. These probes are conjugated with galactosyl-human serum albumin (hGSA) or glucosyl-human serum albumin (glu-HSA), which are commonly used to target H-type lectins, including the β-D-galactose receptor. Fluorescence was only turned ON after internalization by cancer cells because fluorescence was quenched through the connection with the albumin protein. Interestingly, these two different probes were excited by a single wavelength of near 500 nm at a time and performed for detection of ovarian cancer cells and animals containing tumors, verified by red fluorescent protein (RFP) tumor labeling method. Similarly, in another paper, they reported a fluorescent detection method for peritoneal ovarian cancer metastases using bacteriochlorin-based dye, named as NMP1 [70]. They used galactosyl human serum albumin (hGSA) for targeting lectin receptors expressed on. Fluorescence of the conjugated complex was quenched. After internalization of the fluorophore, it showed

Table 4
Conjugation of fluorophores and biomarker-specific ligands for bioimaging of ovarian cancer.

Fluorophore	Ligand	Target	EX/EM (nm/nm)	Disease	Ref
Cyanine	folate	Folate receptor	630/700	Ovarian cancer	[62]
Rhodamine X	avidin	lectin	532/575	ovarian cancer cell	[63]
BODIPY	ABT-199	Bcl-2	488/505–540	human ovary carcinoma (OVCA-429 cell)	[64]
Si-Rhodamine	Olaparib	PARP-1/2	653/678	human ovary carcinoma (OVCA-429 cell), Human fibrosarcoma cell line (HT1080)	[65]
BODIPY	GSH	γ-Glutamyltranspeptidase	450/580–600	Ovarian Cancer	[66]
Rhodamine	z-Phe-Arg	Cathepsin B/L	497/521	Ovarian Cancer	[67]
Rhodamine	hGSA	D-galactose receptor	470/500–550	Ovarian Cancer	[68]
Bacteriochlorin	hGSA, glu-HSA	H-type lectins including the β-D-galactose receptor	503–555/716–823	Ovarian cancer	[69]
Bacteriochlorin	hGSA	lectin receptors	671–705/750	peritoneal ovarian cancer metastases	[70]
Fluorescein	folate	Folate receptor	495/520	Ovarian cancer of patients (Clinical study)	[71]

fluorescence turn-ON in ovarian cancer cells. Interestingly, this probe can be excited with two different wavelengths, both visible and NIR wavelength. This probe was capable of detecting 75% of all peritoneal lesions and 91% of lesions ~0.8 mm or greater in diameter.

γ-Glutamyltranspeptidase has been studied with regards to the metabolism of malignant cells metabolism which require a significant amount of cysteine. Cysteine can be generated by γ-glutamyltranspeptidase from glutathione (GSH) [74]. Fan and colleagues developed enzyme-triggered fluorescent *in situ*-targeting probes for γ-glutamyltranspeptidase in ovarian cancer [66]. They conjugated a BODIPY fluorescent dye with GSH for targeting γ-glutamyltranspeptidase and ovarian cancer cells. They demonstrated remarkable potential for differentiating between ovarian cancer cells and normal cells.

Urano et al. reported using a dipeptide ligand conjugated with hydroxymethylrhodamine green (HMRG), a derivative of the Rhodamine fluorophore [67]. Cathepsin is a cysteine protease which has been known to be overexpressed in various cancer cells including ovarian cancer cells [75–79]. To target cathepsin B/L, they selected a specific ligand group, Z-Phe-Arg, (Z means carboxybenzyl), and connected this with HMRG via a peptide bond which can be cleaved by the cathepsin B/L enzyme in ovarian cancer cell. While fluorescence from the conjugated form was quenched, fluorescence after cleavage displayed turn-ON, which is an excellent strategy for the selective detection of cancer cells. They demonstrated the fluorescent detection potential of their dye on ovarian cancer cells with a high tumor-to-background ratio.

Weissleder et al. reported using fluorescent CID to detect human ovary carcinomas [64]. For this application, they attempted to probe B-cell lymphoma 2 (Bcl-2), anti-apoptotic protein using a conjugated molecule between BODIPY and ABT-199. ABT-199 has been known as a Bcl-2 inhibitor and shows high binding affinity to Bcl-2. They successfully traced ABT-199 movement and imaged the ovary carcinoma. In addition, their group developed another silicon-coordinated Rhodamine probe to image human ovary carcinoma (OVCA-429 cell), the human fibrosarcoma cell line (HT1080) [65]. They targeted PARP 1 using an olaparib drug ligand conjugated with Si-Rhodamine fluorophore synthesized *de novo*. Olaparib is an inhibitor of PARP 1, a protein related to repairing protein or DNA damage and programed cell death. Using this approach, they demonstrated the behavior of olaparib and its selective imaging potential in the cancer cell.

As an example of clinical study, Ntziachristos and co-work group reported intraoperative ovarian cancer imaging using a conjugated FITC with folate [71]. Folate-FITC, 0.1 mg/kg, was injected intravenously to each patient and monitored by intraoperative multispectral imaging system during surgery. They showed targeted fluorescence imaging is beneficial in staging and debulking surgery for ovarian cancer, representing that technique did not induce unwanted interference with standard surgical process.

3.5. Lymphoma

Conjugation methods between fluorophores and ligands in bioimaging strategies of lymphomas are listed in Table 5. As ligands, functional small molecules, not proteins were employed (Table 5), and these were then conjugated with commercial fluorophores; BODIPY, NIR cyanine dyes.

It has been known that integrin α4β1, a heterodimeric cell surface receptor, is usually related to lymphocyte trafficking and homing in normal adult cells. However, integrin α4β1 can be changed into a highly-activated conformation in cancerous cells, specifically T- and B-cell lymphomas [83,84]. Lam and coworkers attempted to probe this receptor using a specific ligand, 2-arylaminobenzothiazole peptide-mimetic antagonist which is linked with a Cy5.5 NIR fluorophore [85]. This conjugated probe displayed good potency for imaging cancerous lymphocytes in a mouse.

Bruton's tyrosine kinase (BTK), non-receptor tyrosine kinase, is usually related to B cell development, and multiple antiapoptotic signaling pathways [86]. However, it has been elucidated that BTK is highly expressed in malignant cells [87]. Weissleder and colleagues developed a specific probing system connected with the BTK inhibitor, ibrutinib [81]. Their group conjugated ibrutinib and a commercial BODIPY dye for specific probing of BTK in lymphoma cells. The results suggest a high probing potency in non-Hodgkin's B cell lymphomas (Toledo cells) and human epithelial fibrosarcoma cells (HT1080).

Yang and colleagues attempted to probe Non-Hodgkin's lymphoma (NHL) [82]. They selected the CD20 antigen as the target, a protein specifically generated in B cell lymphocytes and the majority of non-Hodgkin's lymphomas. The antibody obinutuzumab, which has affinity for CD20, was conjugated to Cy7, an NIR fluorophore. This conjugated probe was tested in mice with Raji tumors overexpressing CD20, and displayed good uptake in tumor and target specificity.

3.6. Prostate cancer

Conjugation methods between biomarker-specified ligands and fluorophores in a prostate cancer are presented in Table 6. Interestingly, prostate-specific antigens were employed for specific targets. Ligands included antibodies, proteins, or small molecules and these were then connected with NIR fluorescent probes.

More specifically, prostate-specific membrane antigen (PSMA) is a specific biomarker expressed in prostate cancer cells [88]. The Berkman group developed a low molecular weight NIR fluorescent probing system [88]. They employed CTT-54.2, a PSMA inhibitor as a ligand and conjugated this with a Cy5.5 NIR fluorophore. They demonstrated specific selective labeling in PSMA-positive prostate cancer cells, LNCaP cells and PC-3 cells.

Frangioni and co-work group developed a new type of zwitterionic NIR fluorophores, ZW800-1, and employed the probe in bioimaging prostate cancer [35]. They conjugated ZW800-1 with a rabbit human α-methylacyl-CoA racemase (AMACR)-specific primary antibody to image human tumor-containing tissues which were prepared from prostatectomies. The group was able to obtain prostate imaging with a high signal to background ratio, which was verified by hematoxylin and eosin staining.

Table 5
Conjugation of fluorophores and biomarker-specific ligands for bioimaging of lymphoma.

Fluorophore	Ligand	Target	EX/EM (nm/nm)	Disease	Ref
Cy5.5	2-Arylaminobenzothiazole peptidomimetic antagonist	Integrin α4β1	–	T- and B-cell lymphomas	[80]
BODIPY	Ibrutinib	Bruton's tyrosine kinase	488/505–540	non-Hodgkin's B cell lymphoma (Toledo cell) Human Epithelial fibrosarcoma cell	[81]
Cy7	Obinutuzumab	CD20 antigen	750/780	Non-Hodgkin's lymphoma	[82]

Table 6
Conjugation of fluorophores and biomarker-specific ligands for bioimaging of prostate cancer.

Fluorophore	Ligand	Target	EX/EM (nm/nm)	Disease	Ref
Cy5.5	CTT-54.2	PSMA	633/670	Prostate cancer	[88]
ZW800-1	AMACR antibody	AMACR	800	Prostate cancer cell	[35]
IR780	–	–	633/780	Prostate cancer cell	[89]
IRDye 800CW	ACPH	PSMA	774/792	Prostate cancer	[90,91]
IR783	–	OATP1B3	633/650	Prostate cancer	[92,93]
IRDy800CW Cy5.5	PSMA-1	PSMA	–	Prostate cancer	[94]
ICG	–	–	690–780/790	Prostate cancer (Clinical study)	[95]

In addition, Pomper group also reported developing a fluorescent imaging probe based on PSMA [90]. They synthesized a specific ligand to target PSMA, 2-(3-[5-[7-(5-amino-1-carboxy-pentylcarbamoyl)-heptanoylamino]-1-carboxy-pentyl]-ureido)-pentanedioic acid (ACPH), which is conjugated with an IRDye 800CW NIR fluorescent probe. This probe displayed at least 10 times higher intensity in PSMA-expressing PC3-PIP vs. PSMA-negative PC3-flu tumors *in vivo*.

Intriguingly, IR-780 iodide, a lipophilic dye, can accumulate selectively in breast cancer cells and drug-resistant human lung cancer cells without any specific ligand [96]. Yuan et al. employed this specific IR-780 iodide dye to image prostate cancer [89]. They mentioned that cell proliferation was inhibited in a dose-dependent manner and the uptake of the fluorophore was mediated by OATP1B3, one of the organic anion-transporting peptides. They were able to monitor the prostate cancer cell selectively in PC-3 cells and prostate cancer xenografts in mice using this NIR probe without a specific ligand.

In addition, Yuan group also introduced an IR783-based prostate tumor imaging method [92]. Interestingly, without any specific conjugation ligands, they were able to obtain selective fluorescent imaging in PC-3, DU-145 and LNCaP human prostate cancer cells. They elucidated that the cellular uptake of IR783 is mediated by OATP1B3, which was verified by utilizing various kinds of uptake inhibitors.

Basilion et al. developed a new technique using IRDye 800CW and a Cy5.5 NIR fluorescent probe for imaging prostate cancer cells [94]. They employed a PSMA-detecting ligand, PSMA-1; Glu-CO-Glu'-Amc-Ahx-Glu-Glu-Glu-Lys-NH_2. Conjugation of this ligand with an NIR fluorophore displayed selective binding affinity to prostate cancer cells in *in vitro* and *in vivo* studies, verified by competitive binding and uptake studies.

As a clinical study, there is a report about fluorescence-guided SLN dissection. Jeschke group attempted to visualize the lymph node and its pathway in real time using ICG fluorophore [95]. ICG solution (2.5 mL, 0.1 mg/mL) was injected into each prostatic lobe. In the first three patients, the dye was administered intra-operatively to display initial flooding of the lymphatic vessels, in which the time interval until dissection was 5–10 min. In other cases, ICG solution was injected directly before the patient is scrubbed and draped, in which the time interval until dissection was 30 min. They were able to remove 582 lymph nodes (median 22, range 11–36) successfully, which is strongly correlated with the result by the standard radio-guided method. They mentioned that the fluorescence-guided technique appears to be effective and easy to dissect sentinel lymph node.

3.7. Other cancers and cancer-related biological targets

Various probing strategies for other cancers or cancer-related molecules are presented in Table 7. While cRGD displayed broad utility for imaging in various cancers including melanoma cells as

Table 7
Conjugation of fluorophores and biomarker-specific ligands for bioimaging of other cancers or cancer-related targets.

Fluorophore	Ligand	Target	EX/EM (nm/nm)	Disease	Ref
ITCC	HSA, Transferrin	Cellular surface receptor for endocytosis via EPR effect	690/740	HT29 human colon cancer cell	[97]
Cy5	RAFT-c(RGDfK)$_4$	αvβ3 integrin	633/-	Tumor engrafted in human embryonic kidney cells HEK293(β3)	[98]
IR786	Hoechst	Extracellular DNA	745/820	Necrosis generated from a myocardial infarction	[99]
Cy5.5	(AEEA)$_1$-YHWYGYTPQNVI-amide	EGFR	670/700	Brain tumor	[100]
TPE	AP2H (IHGHHIISVG)	LAPTM4B	330/350–650	HepG2 cells, BEL 7402 cells, HeLa cells, and Chang liver cells	[101]
Si-Rhodamine	Ibrutinib	Bruton's tyrosine kinase	653/678	Human fibrosarcoma cell line (HT1080)	[102]
zinc phthalocyanine	lactose	Hepatic	asialoglycoprotein (ASGP) receptors	625/700	Liver cancer cell [103]
ICG	–	–	775/810	Live cancer (Clinical study)	[104]
IRDye700DX	panitumumab	EGFR	670/665–740	Acute Necrotic Cancer Cell	[105]
Rhodamine	indomethacin	cyclooxygenase-2 (COX2)	581/603	Non-melanoma skin cancer	[106]
IDCC	Octreotate	receptors for somatostatin	740/780–900	Neuroendocrine tumors	[107]
IDCC	dFMFdWK	receptors for somatostatin	740/780–900	Neuroendocrine tumors	[107]
ITCC	Octreotate	receptors for somatostatin	740/780–900	Neuroendocrine tumors	[107]
IRDye 800CW	MC1RL	MC1R	790/	malignant melanoma	[108,109]
Cy5	MC1RL	MC1R	790/	malignant melanoma	[108]
ZW800-1	cRGD	Integrin αvβ3	/800	melanoma cell	[35]

well as in lung cancer, peptide ligands showed high specificity to target ligands although they are relatively small relative to antibodies. Interestingly, there is a report about a 'RAFT' vector molecule, which can connect one fluorophore and four target specific-ligands which improves signal to background ratio.

It has been known that transferrin is overexpressed in tumor cells [41,110], and can be targeting for tumor imaging or drug delivery [111,112]. Licha group reported the development of a transferrin-connected NIR probe [97]. Transferrin was adopted as a specific ligand for the transferrin receptor found on tumor cell surfaces and was linked with ITCC derivatives as fluorophores. This conjugated fluorophore showed good uptake and imaging potential in HT29 human colon cancer cells.

Coll and colleagues introduced a novel vector system for connection between a fluorophore and a specific ligand for tumor imaging [98]. They adopted the cyclic decapeptide vector RAFT discussed above and conjugated four c(RGDfK) ligands and a Cy 5 NIR probe. Each c(RGDfK) ligand was targeted for αVβ3 integrin. This probe showed strong potential as a probe for αVβ3-positive-tumors in human embryonic kidney cells, HEK293 (β3).

Murthy et al. reported using an imaging strategy for necrotic tissue by detecting exposed extracellular DNA fragments using a double-stranded oligonucleotide (sense strand, 5′-AGTTGAGGGGACTTTCCCAGGC-3) [99]. They employed Hoechst, a staining dye that has been known to show high affinity for DNA [113,114]. They conjugated Hoechst with an IR786 NIR dye, and monitored tissue necrosis *in vivo* after a myocardial infarction, and tissue necrosis *in vivo* caused by LPS-GalN-induced sepsis and demonstrated probing potency of this conjugated molecule.

The Basilion group attempted to probe orthotopic brain tumors overexpressing EGFR, noninvasively [100]. They synthesized a specific peptide ligand, $(AEEA)_1$-YHWYGYTPQNVI-amide, to target EGFR, and conjugated this with Cy5.5 NIR fluorophores. They observed good binding and cellular uptake of Cy5.5-GE11-conjugated dye in glioblastoma cells overexpressing EGFR *in vitro*, and glioblastoma-derived orthotopic brain tumors *in vivo*.

It has been known that the lysosomal protein transmembrane 4 beta (LAPTM4B) is overexpressed in many types of solid tumors, including carcinomas of the liver, lung, breast, cervix, and ovary [115–118]. Zhang and colleagues introduced fluorescent tumor markers in live cancer cells using tetraphenylethylene (TPE), an aggregation-induced emission fluorophore [101]. They employed the small peptide, AP2H (IHGHHIISVG), which targets the hydrophilic extracellular loop (EL2, PYRDDVMSVN) of LAPTM4B. While the conjugated fluorophore did not emit fluorescence because of a quenching mechanism related to the internal conversion mechanism, high fluorescence was displayed after binding of this probe with a target molecule by stopping the internal conversion for dequenching. They demonstrated that this probe has good imaging potential in HepG2 BEL 7402, HeLa, and Chang liver cells.

Btk is a nonreceptor tyrosine kinase, relating to B-cell proliferation, activation, macrophage signaling, and ischaemic brain injury. It is also highly expressed in B-cell malignancies, myeloma, and non-Hodgkin's lymphoma [119–122]. The Weissleder group developed a fluorescent probe targeting for Btk in the human fibrosarcoma cell line (HT1080) [102]. For targeting cellular Btk, they employed ibrutinib, a Btk inhibitor, and conjugated this with a Si-rhodamine fluorophore to make CID with *de novo* synthesis. This CID displayed good potential for identifying the cellular location of Bkt and the cellular distribution of ibrutinib, verified with green fluorescent protein (GFP) cellular expression in HT1080 cells.

The Liu group describe an organometallic NIR fluorescent probe based on zinc (II) phthalocyanine in liver cancer, prepared through *de novo* synthesis [103]. For targeting hepatic asialoglycoprotein (ASGP) receptors, they employed lactose as a ligand. ASGP has been known to be overexpressed in hepatocyte membranes, the endothelial membrane of the liver [123–125]. This lactose-conjugated NIR probe displayed potential as a good diagnostic tool in mouse models of liver cancer.

The Kobayashi group attempted to conjugate an NIR fluorophore and an antibody for probing *in vivo* acute necrotic cancer cell death [105]. An IRDye700DX NIR probe was connected with panitumumab, an antibody against EGFR. Interestingly, they described that necrosis can be generated by NIR radiation if the conjugated fluorophore of the antibody- IRDye700DX is bound with EGFR. By using FLIM, necrosis induced by exposal of NIR light was successfully detected using this probe in A431 tumor cells and mouse models of tumorigenicity.

Cyclooxygenase-2 (COX-2) is known to be highly expressed in inflamed and various neoplastic tissues, including colon, prostate, breast, pancreas, lung, and skin [106,126,127]. Contag et al. described a molecular fluorescent probe, fluorocoxib A, which is a combined probe of Rhodamine and indomethacin, for molecular imaging of Non-melanoma skin cancer (NMSC) [106]. Indomethacin can specifically bind to COX-2. When using fluorocoxib A on basal cell carcinoma (BCC) allograft models and the spontaneous P14 mouse model, they obtained good fluorescent detection results. The sensitivity was 88% and the specificity was 100% in macroscopic tumors.

The somatostatin receptor is overexpressed in many tumors. Wiedenmann and colleagues attempted to conjugate two types of NIR fluorophores, indodicarbocyanine (IDCC) and ITCC, with three types of ligands; samotostatin-14, octreotate, and M^2M^7-octreotate (dFMFdWK, cysteine-substituted version with methionine) with combinatorial methods [107]. These fluorophore-conjugated ligands showed excellent imaging ability in RIN38/SSTR2 neuroendocrine tumor cells.

From knowledge about the correlation between the conversion of ceramide into sphingomyelin and cancer progression [128], Génisson and coworkers developed a fluorescent probing system using the ceramide transfer (CERT) protein in an ovary mutant cell line [129]. They attempted to conjugate NBD or BODIPY with ceramide to detect CERT protein and demonstrated good imaging potential in ovary mutant cell line.

Vagner and colleagues employed a fluorescent imaging probe for melanoma [108]. They developed a peptidomimetic ligand (MC1RL) for targeting the melanocortin 1 receptor (MC1R), known to be overexpressed in most human melanoma metastases. They conjugated this ligand with the NIR probes, IRDye 800CW and Cy5, and used this to image nude mice bearing bilateral subcutaneous A375 xenograft tumors with low MC1R expression and engineered A375/MC1R tumors with high receptor expression. These probes displayed high signal to background ratio in engineered A375/MC1R tumors with high receptor expression.

As a clinical application, ICG was utilized in liver cancer imaging without conjugating with any specific ligands. Kokudo and co-research group delineated real-time identification of liver cancer using ICG-based fluorescence [104]. They injected ICG (0.5 mg/kg/body) intravenously to 37 patients with hepatocellular carcinoma (1–7 days before surgery) and 12 patients with metastasis (1–14 days before surgery) of colorectal carcinoma before liver resection. They mentioned surgery should be performed after 2 days from ICG injection to obtain a good lesion-to-liver contrast for fluorescent signal assessment tests. This study displayed good imaging potential in small and grossly unidentifiable liver cancers in real time.

3.8. Perspectives

During our literature searches regarding cancer imaging, we found some interesting trends about fluorophores and ligands.

Firstly, as shown here, fluorophores can be broadly classified into NIR or non-NIR probes. While non-NIR probes showed good potential for cellular imaging, NIR probes exhibited broader utility for use in animal tissues due to their deeper penetration properties. Interestingly, almost all fluorophores: BODIPY, cyanine-based dyes, Rhodamine derivatives, and Fluorescein, were commercial because they may be convenient to use and are stable under cellular conditions. However, considering various conditions in cancer cells, it is necessary to develop new kinds of fluorophores which are superior to commercial ones. It is expected that the development of more advanced fluorophores will help obtain better cancer imaging and increase the accuracy of cancer diagnosis.

Considering ligands, there are some trends among various proteins, peptides, and small organic molecules; from big protein molecules to simplified small organic ligands, and from narrowly-targeted to broadly-targeted ligands. Although antibodies or receptor-binding proteins showed quite good results, they are relatively hard to handle and showed relatively high background signal; they should be handled under specific pH conditions and temperatures with care [9]. Peptide-based ligands exhibited medium potency, while relatively small size (compared to the whole protein) and high specificity to target molecules are advantages, inconvenient handling is still a significant disadvantage. Small organic molecule-based ligands are more convenient than protein or peptide-based ligands, but their specificity must be improved. However, drug-based ligands are an exception to this rule and display high specificity. In addition, ligands targeting for receptors which are commonly expressed in several cancers may have broader application. However, they may exhibit a relatively low signal to background ratio because the receptors may also be expressed in normal cells although in some cases the expression levels are low relative to cancer cells. Contrary to broad-spectrum ligands, narrow spectrum ligands for targeted specific cancer antigen such as PSMA can be expected to generate a relatively high signal to background ratio.

For selection of an appropriate ligand for a specific cancer, various conditions such as; cell/tissue types, target materials, effectiveness of ligand preparation, selectivity, and sensitivity, should be considered. We would like to recommend two types of ligands; *peptide-based* and *drug-based* ligands. In particular, drug-based ligands have really high potential because they can be easily synthesized massively using systematic chemical synthesis. Most of all, they show high selectivity and sensitivity for enzyme which are involved in various cancers since they can interact stereochemically with the active site of target enzyme in a strict host-guest interaction manner, consisting of hydrogen bonds, ionic interactions, and van der Waals interactions. Additionally, peptide-based ligands have really good potential due to high selectivity and sensitivity with relatively easy systematic peptide preparation method. Peptide-based ligand can be considered as a simplified version of antibody. They can be prepared by mimicking the core active peptide sequence of antibody or the SELEX method from using virus screening [10]. Interaction kinetics of peptide-based ligand is based on the interaction between antibody and antigen.

Based on these various attempts, development of conjugated fluorescent molecules with a small sized ligand can have high potency and improve cancer diagnosis and cancer therapy, including surgery with few side effect.

With regard to clinical applications for *in vivo* human tumor imaging, mainly two fluorophores have been utilized; ICG and fluorescein, which are approved for use in clinics by USA Food and Drug Administration (FDA). In almost clinical studies, ICG was applied to image human cancers in the absence of a target-specific ligand. Specific ligand-conjugated ICG will provide more efficient and plentiful information for cancer diagnosis and therapy. Although a number of fluorophores have been developed, few fluorophores reached to clinical utilization. Therefore, we want to suggest that clinical cancer imaging using the ligand-conjugated fluorophores are in an early stage, and there are a lot of potentials for cancer diagnosis and therapy.

4. Conclusions

Herein, we reviewed recent conjugation strategies between organic or organometallic fluorophores and specific ligands which are for cancer-specific or cancer-related targets. Various conjugated fluorophores show good potential as fluorescent imaging options in cancer cells or animal tissues via adoption of fluorescent principles; these include Pet, FRET, and FLIM. In particular, NIR fluorophores, such as cyanine derivatives, showed high potency in aqueous biological circumstances due to their ability to penetrate deeply into animal tissues. The non-NIR fluorophores; BODIPY, Rhodamine, Fluorescein, were utilized only for *cellular* imaging due to its high intensity, and easy handling. Also, various ligand molecules, from proteins to small organic molecules including HSA, receptor binding proteins, antibodies, enzymes, small-sized peptides, aptamers, and organic molecules, were utilized to target various cancer-specific biomarkers. Considering a variety of factors including the wavelength of fluorophores, fluorescent techniques, ligand sizes, ligand specificity, it is essential to develop additional fluorophores, ligands and to find cancer-specific biomarker, which may then contribute to improved cancer therapies.

Acknowledgements

This work was supported by the National Research Foundation of Korea Grant funded by the Korean Government (NRF-2013R1A1A1076020).

Transparency document

Transparency document related to this article can be found online at http://dx.doi.org/10.1016/j.cbi.2016.02.006.

Abbreviations

AMACR	α-methylacyl-CoA racemase
BCC	basal cell carcinoma
BHQ3	black hole quencher 3
BMVC	3,6-bis(1-methyl-4-vinylpyridinium) carbazole diiodide
C-CPE	*C*-terminal partial fragment of *Clostridium perfringens* enterotoxin
CDI	carbonyl diimidazole
CERT	ceramide transfer
CID	companion imaging drug
COX-2	cyclooxygenase-2
cRGD	cyclic arginine-glycine-aspartic acid peptide
CT	computed tomography
DCC	*N*,*N*′-Dicyclohexylcarbodiimide
DIC	*N*,*N*′-Diisopropylcarbodiimide
DMBA	7,12-dimethyl-1,2-benzanthracene
DSC	*N*,*N*′-disuccinimidyl carbonate
EDC	1-ethyl-3-(3-dimethylaminopropyl)carbodiimide
EGF	epithermal growth factor
EGFR	epithermal growth factor receptor
ELISA	enzyme-linked immunosorbent assay
EM	emission wavelength
EX	excitation wavelength
FITC	Fluorescein isothiocyanate
FLIM	fluorescent lifetime imaging

FRET	Förster resonance energy transfer
Glut	glucose transporter
GROs	guanine-rich oligonucleotides
GSH	glutathione
MEMS	HyperEye Medical System
HER	human epidermal growth factor receptor
hGSA	human galactosyl serum albumin
HSA	human serum albumin
ICG	indocyanine green
IL	interleukin
IL-11Rα	interleukin 11 receptor alpha-chain
ITCC	indotricarbocyanine
MC1R	melanocortin 1 receptor
MC1RL	ligand for melanocortin 1 receptor
MSA	neomannosyl human serum albumin
NBD	7-nitro-1,2,3-benzadiazole
NHS	*N*-hydroxysuccinimide
NIR	near infrared
NMR	nuclear magnetic resonance
NMSC	Non-melanoma skin cancer
NRP-1	neuropilin-1
PARP	poly(ADP-ribose) polymerase
PECAM 1	platelet/endothelial cell adhesion molecule 1
PeT	photoinduced electron transfer
PET	positron emission tomography
SLN	sentinel lymph node
SPECT	single-photon emission computerized tomography
TLR	Toll-like receptor
uMUC-1	mucin-1 tumor antigen

References

[1] S. Luo, E. Zhang, Y. Su, T. Cheng, C. Shi, A review of NIR dyes in cancer targeting and imaging, Biomaterials 32 (2011) 7127–7138.
[2] Z. Li, T.-P. Lin, S. Liu, C.-W. Huang, T.W. Hudnall, F.P. Gabbai, P.S. Conti, Rapid aqueous [18F]-labeling of a bodipy dye for positron emission tomography/fluorescence dual modality imaging, Chem. Commun. 47 (2011) 9324–9326.
[3] H. Kobayashi, M.R. Longmire, M. Ogawa, P.L. Choyke, Rational chemical design of the next generation of molecular imaging probes based on physics and biology: mixing modalities, colors and signals, Chem. Soc. Rev. 40 (2011) 4626–4648.
[4] I. Atallah, C. Milet, J.-L. Coll, E. Reyt, C.A. Righini, A. Hurbin, Role of near-infrared fluorescence imaging in head and neck cancer surgery: from animal models to humans, Eur. Arch. Oto-Rhino-Laryngol. 272 (2015) 2593–2600.
[5] A. Motekallemi, H.-R. Jeltema, J.D.M. Metzemaekers, G.M. van Dam, L.M.A. Crane, R.J.M. Groen, The current status of 5-ALA fluorescence-guided resection of intracranial meningiomas-a critical review, Neurosurg. Rev. 38 (2015) 619–628.
[6] T. Murakami, Y. Hiroshima, Y. Zhang, M. Bouvet, T. Chishima, K. Tanaka, I. Endo, R.M. Hoffman, Improved disease-free survival and overall survival after fluorescence-guided surgery of liver metastasis in an orthotopic nude mouse model, J. Surg. Oncol. 112 (2015) 119–124.
[7] H.-A. Leroy, M. Vermandel, J.-P. Lejeune, S. Mordon, N. Reyns, Fluorescence guided resection and glioblastoma in 2015: a review, Lasers Surg. Med. 47 (2015) 441–451.
[8] J. Parrish-Novak, E.C. Holland, J.M. Olson, Image-guided tumor resection, Cancer J. 21 (2015) 206–212.
[9] H. Kobayashi, M. Ogawa, R. Alford, P.L. Choyke, Y. Urano, New strategies for fluorescent probe design in medical diagnostic imaging, Chem. Rev. 110 (2010) 2620–2640.
[10] M. Vendrell, D. Zhai, J.C. Er, Y.-T. Chang, Combinatorial strategies in fluorescent probe development, Chem. Rev. 112 (2012) 4391–4420.
[11] G.T. Hermanson, Bioconjugate Techniques, third ed., Acdemic Press, 2013.
[12] M.S.T. Gonçalves, Fluorescent labeling of biomolecules with organic probes, Chem. Rev. 109 (2009) 190–212.
[13] J. Jose, K. Burgess, Benzophenoxazine-based fluorescent dyes for labeling biomolecules, Tetrahedron 62 (2006) 11021–11037.
[14] H. Sahoo, Fluorescent labeling techniques in biomolecules: a flashback, RSC Adv. 2 (2012) 7017–7029.
[15] B. Valeur, Molecular fluorescence: principles and applications, Wiley-VCH, Weinheim, 2001.
[16] A. Loudet, K. Burgess, BODIPY dyes and Their derivatives: syntheses and spectroscopic properties, Chem. Rev. 107 (2007) 4891–4932.
[17] P. Gobbo, P. Gunawardene, W. Luo, M.S. Workentin, Synthesis of a toolbox of clickable rhodamine B derivatives, Synlett 26 (2015) 1169–1174.
[18] H. Aviv, S. Harazi, D. Schiff, Y. Ramon, Y.R. Tischler, Synthesis of an amphiphilic rhodamine derivative and characterization of its solution and thin film properties, Thin Solid Films 564 (2014) 86–91.
[19] D.A. Weiss, C.H. Jaworek-Lopes, Microwave synthesis of fluorescein and selected derivatives of fluorescein, Abstr. Pap. Am. Chem. Soc. 245 (2013).
[20] M.P. Cook, S. Ando, K. Koide, One-step synthesis of a fluorescein derivative and mechanistic studies, Tetrahedron Lett. 53 (2012) 5284–5286.
[21] P. Ghosh, J. Zhang, Z.-Z. Shi, K. Li, Synthesis and evaluation of an imidazole derivative-fluorescein conjugate, Bioorg. Med. Chem. 21 (2013) 2418–2425.
[22] J. Gu, U.R. Anumala, R. Heyny-von Haussen, J. Hoelzer, V. Goetschy-Meyer, G. Mall, I. Hilger, C. Czech, B. Schmidt, Design, synthesis and biological evaluation of trimethine cyanine dyes as fluorescent probes for the detection of tau fibrils in Alzheimer's disease brain and olfactory epithelium, ChemMedChem 8 (2013) 891–897.
[23] X.H. Zhang, Q. Liu, H.J. Shi, L.Y. Wang, Y.L. Fu, X.C. Wei, L.F. Yang, Synthesis, spectral properties of cell-permeant dimethine cyanine dyes and their application as fluorescent probes in living cell imaging and flow cytometry, Dyes Pigm. 100 (2014) 232–240.
[24] A.P. de Silva, H.Q.N. Gunaratne, T. Gunnlaugsson, A.J.M. Huxley, C.P. McCoy, J.T. Rademacher, T.E. Rice, Signaling recognition events with fluorescent sensors and switches, Chem. Rev. 97 (1997) 1515–1566.
[25] K. Abe, L. Zhao, A. Periasamy, X. Intes, M. Barroso, Non-invasive in vivo imaging of near infrared-labeled transferrin in breast cancer cells and tumors using fluorescence lifetime FRET, PLoS One 8 (2013).
[26] N.P. Galletly, J. McGinty, C. Dunsby, F. Teixeira, J. Requejo-Isidro, I. Munro, D.S. Elson, M.A.A. Neil, A.C. Chu, P.M.W. French, G.W. Stamp, Fluorescence lifetime imaging distinguishes basal cell carcinoma from surrounding uninvolved skin, Br. J. Dermatol. 159 (2008) 152–161.
[27] O.T. Okusanya, E.M. DeJesus, J.X. Jiang, R.P. Judy, O.G. Venegas, C.G. Deshpande, D.F. Heitjan, S. Nie, P.S. Low, S. Singhal, Intraoperative molecular imaging can identify lung adenocarcinomas during pulmonary resection, J. Thorac. Cardiovasc. Surg. 150 (2015) 28–35.e1.
[28] A. Petrovsky, E. Schellenberger, L. Josephson, R. Weissleder, A. Bogdanov, Near-infrared fluorescent imaging of tumor apoptosis, Cancer Res. 63 (2003) 1936–1942.
[29] D. Citrin, A.K. Lee, T. Scott, M. Sproull, C. Ménard, P.J. Tofilon, K. Camphausen, In vivo tumor imaging in mice with near-infrared labeled endostatin, Mol. Cancer Ther. 3 (2004) 481–488.
[30] E. Garanger, D. Boturyn, Z. Jin, P. Dumy, M.-C. Favrot, J.-L. Coll, New multifunctional molecular conjugate vector for targeting, imaging, and therapy of tumors, Mol. Ther. 12 (2005) 1168–1175.
[31] T.-Y. Tseng, Z.-F. Wang, C.-H. Chien, T.-C. Chang, In-cell optical imaging of exogenous G-quadruplex DNA by fluorogenic ligands, Nucleic Acids Res. 41 (2013) 10605–10618.
[32] M. Ogawa, N. Kosaka, M.R. Longmire, Y. Urano, P.L. Choyke, H. Kobayashi, Fluorophore-quencher based activatable targeted optical probes for detecting in vivo cancer metastases, Mol. Pharm. 6 (2009) 386–395.
[33] Y. Urano, D. Asanuma, Y. Hama, Y. Koyama, T. Barrett, M. Kamiya, T. Nagano, T. Watanabe, A. Hasegawa, P.L. Choyke, H. Kobayashi, Selective molecular imaging of viable cancer cells with pH-activatable fluorescence probes, Nat. Med. 15 (2009) 104–109.
[34] X. He, M.-H. Na, J.-S. Kim, G.-Y. Lee, J.Y. Park, A.S. Hoffman, J.-O. Nam, S.-E. Han, G.Y. Sim, Y.-K. Oh, I.-S. Kim, B.-H. Lee, A novel peptide probe for imaging and targeted delivery of liposomal doxorubicin to lung tumor, Mol. Pharm. 8 (2011) 430–438.
[35] H.S. Choi, S.L. Gibbs, J.H. Lee, S.H. Kim, Y. Ashitate, F. Liu, H. Hyun, G. Park, Y. Xie, S. Bae, M. Henary, J.V. Frangioni, Targeted zwitterionic near-infrared fluorophores for improved optical imaging, Nat. Biotechnol. 31 (2013) 148–153.
[36] H. Tang, C. Xing, L. Liu, Q. Yang, S. Wang, Synthesis of amphiphilic polythiophene for cell imaging and monitoring the cellular distribution of a cisplatin anticancer drug, Small 7 (2011) 1464–1470.
[37] Y. Oh, Y.-S. Lee, Y.H. Quan, Y. Choi, J.M. Jeong, B.-M. Kim, H.K. Kim, Thoracoscopic color and fluorescence imaging system for sentinel lymph node mapping in porcine lung using indocyanine green-neomannosyl human serum albumin: intraoperative image-guided sentinel nodes navigation, Ann. Surg. Oncol. 21 (2014) 1182–1188.
[38] S.-I. Yamashita, K. Tokuishi, K. Anami, M. Miyawaki, T. Moroga, M. Kamei, S. Suehiro, K. Ono, S. Takeno, M. Chujo, S. Yamamoto, K. Kawahara, Video-assisted thoracoscopic indocyanine green fluorescence imaging system shows sentinel lymph nodes in non-small-cell lung cancer, J. Thorac. Cardiovasc. Surg. 141 (2011) 141–144.
[39] J.T. Alander, I. Kaartinen, A. Laakso, T. Pätilä, T. Spillmann, V.V. Tuchin, M. Venermo, P. Välisuo, A review of indocyanine green fluorescent imaging in surgery, Int. J. Biomed. Imaging 2012 (2012) 26.
[40] S. Ke, X. Wen, M. Gurfinkel, C. Charnsangavej, S. Wallace, E.M. Sevick-Muraca, C. Li, Near-infrared optical imaging of epidermal growth factor receptor in breast cancer xenografts, Cancer Res. 63 (2003) 7870–7875.
[41] A.A. Phylchenkov, I.I. Slukvin, Y.I. Kudryavets, Preferential coexpression of the functionally active receptors for EGF and transferrin in some human tumor cell lines of the epithelial origin, Exp. Oncol. 22 (2000) 130–134.
[42] Y.B. Kang, W. He, S. Tulley, G.P. Gupta, I. Serganova, C.R. Chen, K. Manova-Todorova, R. Blasberg, W.L. Gerald, J. Massague, Breast cancer bone metastasis mediated by the Smad tumor suppressor pathway, Proc. Natl. Acad. Sci.

U. S. A. 102 (2005) 13909–13914.
[43] M. Lacroix, B. Siwek, P.J. Marie, J.J. Body, Production and regulation of interleukin-11 by breast cancer cells, Cancer Lett. 127 (1998) 29–35.
[44] W. Wang, S. Ke, S. Kwon, S. Yallampalli, A.G. Cameron, K.E. Adams, M.E. Mawad, E.M. Sevick-Muraca, A new optical and nuclear dual-labeled imaging agent targeting interleukin 11 receptor alpha-chain, Bioconjugate Chem. 18 (2007) 397–402.
[45] J. Levi, Z. Cheng, O. Gheysens, M. Patel, C.T. Chan, Y. Wang, M. Namavari, S.S. Gambhir, Fluorescent fructose derivatives for imaging breast cancer cells, Bioconjugate Chem. 18 (2007) 628–634.
[46] A.E. Frees, N. Rajaram, S.S. McCachren III, A.N. Fontanella, M.W. Dewhirst, N. Ramanujam, Delivery-corrected imaging of fluorescently-labeled glucose reveals distinct metabolic phenotypes in murine breast cancer, PLoS One 9 (2014).
[47] A. Maeda, J. Bu, J. Chen, G. Zheng, R.S. DaCosta, Dual in vivo photoacoustic and fluorescence imaging of HER2 expression in breast tumors for diagnosis, margin assessment, and surgical guidance, Mol. Imaging 14 (2015).
[48] G.-K. Feng, R.-B. Liu, M.-Q. Zhang, X.-X. Ye, Q. Zhong, Y.-F. Xia, M.-Z. Li, J. Wang, E.-W. Song, X. Zhang, Z.-Z. Wu, M.-S. Zeng, SPECT and near-infrared fluorescence imaging of breast cancer with a neuropilin-1-targeting peptide, J. Control. Rel. 192 (2014) 236–242.
[49] X. Li, W. Zhang, L. Liu, Z. Zhu, G. Ouyang, Y. An, C. Zhao, C.J. Yang, In vitro selection of DNA aptamers for metastatic breast cancer cell recognition and tissue imaging, Anal. Chem. 86 (2014) 6596–6603.
[50] L. Zhu, H. Wang, L. Wang, Y. Wang, K. Jiang, C. Li, Q. Ma, S. Gao, L. Wang, W. Li, M. Cai, H. Wang, G. Niu, S. Lee, W. Yang, X. Fang, X. Chen, High-affinity peptide against MT1-MMP for in vivo tumor imaging, J. Control. Rel. 150 (2011) 248–255.
[51] T. Reiner, S. Earley, A. Turetsky, R. Weissleder, Bioorthogonal small-molecule ligands for PARP1 imaging in living cells, ChemBioChem 11 (2010) 2374–2377.
[52] U. Toh, N. Iwakuma, M. Mishima, M. Okabe, S. Nakagawa, Y. Akagi, Navigation surgery for intraoperative sentinel lymph node detection using indocyanine green (ICG) fluorescence real-time imaging in breast cancer, Breast Cancer Res. Treat. 153 (2015) 337–344.
[53] J.E. Bugaj, S. Achilefu, R.B. Dorshow, R. Rajagopalan, Novel fluorescent contrast agents for optical imaging of in vivo tumors based on a receptor-targeted dye-peptide conjugate platform, J Biomed Opt. 6 (2001) 122–133.
[54] T. Reiner, J. Lacy, E.J. Keliher, K.S. Yang, A. Ullal, R.H. Kohler, C. Vinegoni, R. Weissleder, Imaging therapeutic PARP inhibition in vivo through bioorthogonally developed companion imaging agents, Neoplasia 14 (2012) 169–177.
[55] H. Li, Y. Li, L. Cui, B. Wang, W. Cui, M. Li, Y. Cheng, Monitoring pancreatic carcinogenesis by the molecular imaging of cathepsin E in vivo using confocal laser endomicroscopy, PLoS One 9 (2014).
[56] A. Neesse, A. Hahnenkamp, H. Griesmann, M. Buchholz, S.A. Hahn, A. Maghnouj, V. Fendrich, J. Ring, B. Sipos, D.A. Tuveson, C. Bremer, T.M. Gress, P. Michl, Claudin-4-targeted optical imaging detects pancreatic cancer and its precursor lesions, Gut 62 (2013) 1034–1043.
[57] H. Amanda Shanks, W.J. Chung, H.-I. Cho, V.E. Moberg, E. Celis, D.L. Morse, J. Vagner, Novel toll-like receptor 2 ligands for targeted pancreatic cancer imaging and immunotherapy, J. Med. Chem. 55 (2012) 9751–9762.
[58] W. Pham, Z. Medarova, A. Moore, Synthesis and application of a water-soluble near-infrared dye for cancer detection using optical imaging, Bioconjugate Chem. 16 (2005) 735–740.
[59] H. Ideo, Y. Hinoda, K. Sakai, I. Hoshi, S. Yamamoto, M. Oka, K. Maeda, N. Maeda, S. Hazama, J. Amano, K. Yamashita, Expression of mucin 1 possessing a 3-sulfated core1 in recurrent and metastatic breast cancer, Int. J. Cancer 137 (2015) 1652–1660.
[60] S. Jain, D. Stroopinsky, L. Yin, J. Rosenblatt, M. Alam, P. Bhargava, R.A. Clark, T.S. Kupper, K. Palmer, M.D. Coll, H. Rajabi, A. Pyzer, M. Bar-Natan, K. Luptakova, J. Arnason, R. Joyce, D. Kufe, D. Avigan, Mucin 1 is a potential therapeutic target in cutaneous T-cell lymphoma, Blood 126 (2015) 354–362.
[61] X. Song, R.D. Airan, D.R. Arifin, A. Bar-Shir, D.K. Kadayakkara, G. Liu, A.A. Gilad, P.C.M. van Zijl, M.T. McMahon, J.W.M. Bulte, Label-free in vivo molecular imaging of underglycosylated mucin-1 expression in tumour cells, Nat. Commun. 6 (2015).
[62] C.H. Tung, Y.H. Lin, W.K. Moon, R. Weissleder, A receptor-targeted near-infrared fluorescence probe for in vivo tumor imaging, Chembiochem 3 (2002) 784–786.
[63] Y. Hama, Y. Urano, Y. Koyama, M. Kamiya, M. Bernardo, R.S. Paik, I.S. Shin, C.H. Paik, P.L. Choyke, H. Kobayashi, A target cell-specific activatable fluorescence probe for in vivo molecular imaging of cancer based on a self-quenched avidin-rhodamine conjugate, Cancer Res. 67 (2007) 2791–2799.
[64] R.J. Giedt, M.M. Sprachman, K.S. Yang, R. Weissleder, Imaging cellular distribution of Bcl inhibitors using small molecule drug conjugates, Bioconjugate Chem. 25 (2014) 2081–2085.
[65] E. Kim, K.S. Yang, R.J. Giedt, R. Weissleder, Red Si-rhodamine drug conjugates enable imaging in GFP cells, Chem. Commun. 50 (2014) 4504–4507.
[66] F. Wang, Y. Zhu, L. Zhou, L. Pan, Z. Cui, Q. Fei, S. Luo, D. Pan, Q. Huang, R. Wang, C. Zhao, H. Tian, C. Fan, Fluorescent in situ targeting probes for rapid imaging of ovarian-cancer-specific gamma-glutamyltranspeptidase, Angew. Chem. Int. Ed. 54 (2015) 7349–7353.
[67] T. Fujii, M. Kamiya, Y. Urano, In vivo Imaging of intraperitoneally disseminated tumors in model mice by using activatable fluorescent small-molecular probes for activity of cathepsins, Bioconjugate Chem. 25 (2014) 1838–1846.
[68] T. Nakajima, K. Sano, K. Sato, R. Watanabe, T. Harada, H. Hanaoka, P.L. Choyke, H. Kobayashi, Fluorescence-lifetime molecular imaging can detect invisible peritoneal ovarian tumors in bloody ascites, Cancer Sci. 105 (2014) 308–314.
[69] T. Harada, K. Sano, K. Sato, R. Watanabe, Z. Yu, H. Hanaoka, T. Nakajima, P.L. Choyke, M. Ptaszek, H. Kobayashi, Activatable organic near-infrared fluorescent probes based on a bacteriochlorin platform: synthesis and multicolor in vivo imaging with a single excitation, Bioconjugate Chem. 25 (2014) 362–369.
[70] V.M. Alexander, K. Sano, Z. Yu, T. Nakajima, P.L. Choyke, M. Ptaszek, H. Kobayashi, Galactosyl human serum albumin-NMP1 conjugate: a near infrared (NIR)-activatable fluorescence imaging agent to detect peritoneal ovarian cancer metastases, Bioconjugate Chem. 23 (2012) 1671–1679.
[71] G.M. van Dam, G. Themelis, L.M.A. Crane, N.J. Harlaar, R.G. Pleijhuis, W. Kelder, A. Sarantopoulos, J.S. de Jong, H.J.G. Arts, A.G.J. van der Zee, J. Bart, P.S. Low, V. Ntziachristos, Intraoperative tumor-specific fluorescence imaging in ovarian cancer by folate receptor-[alpha] targeting: first in-human results, Nat. Med. 17 (2011) 1315–1319.
[72] S.D. Konda, M. Aref, S. Wang, M. Brechbiel, E.C. Wiener, Specific targeting of folate-dendrimer MRI contrast agents to the high affinity fo late receptor expressed in ovarian tumor xenografts, Magn. Reson. Mater. Phys. Biol. Med. 12 (2001) 104–113.
[73] G. Toffoli, C. Cernigoi, A. Russo, A. Gallo, M. Bagnoli, M. Boiocchi, Overexpression of folate binding protein in ovarian cancers, Int. J. Cancer 74 (1997) 193–198.
[74] A. Pompella, V. De Tata, A. Paolicchi, F. Zunino, Expression of gamma-glutamyltransferase in cancer cells and its significance in drug resistance, Biochem. Pharmacol. 71 (2006) 231–238.
[75] T. Gemoll, F. Epping, L. Heinrich, B. Fritzsche, U.J. Roblick, S. Szymczak, S. Hartwig, R. Depping, H.-P. Bruch, C. Thorns, S. Lehr, A. Paech, J.K. Habermann, Increased cathepsin D protein expression is a biomarker for osteosarcomas, pulmonary metastases and other bone malignancies, Oncotarget 6 (2015) 16517–16526.
[76] Z.-Z. Xu, P. Xiu, J.-W. Lv, F.-H. Wang, X.-F. Dong, F. Liu, T. Li, J. Li, Integrin alpha v beta 3 is required for cathepsin B-induced hepatocellular carcinoma progression, Mol. Med. Rep. 11 (2015) 3499–3504.
[77] B. Sobotic, M. Vizovisek, R. Vidmar, P. Van Damme, V. Gocheva, J.A. Joyce, K. Gevaert, V. Turk, B. Turk, M. Fonovic, Proteomic identification of cysteine cathepsin substrates shed from the surface of cancer cells, Mol. Cell. Proteomics 14 (2015) 2213–2228.
[78] L. Zhang, L. Wei, G. Shen, B. He, W. Gong, N. Min, L. Zhang, Y. Duan, J. Xie, H. Luo, X. Gao, Cathepsin L is involved in proliferation and invasion of ovarian cancer cells, Mol. Med. Rep. 11 (2015) 468–474.
[79] W. Zhang, S. Wang, Q. Wang, Z. Yang, Z. Pan, L. Li, Overexpression of cysteine cathepsin L is a marker of invasion and metastasis in ovarian cancer, Oncol. Rep. 31 (2014) 1334–1342.
[80] R.D. Carpenter, M. Andrei, O.H. Aina, E.Y. Lau, F.C. Lightstone, R. Liu, K.S. Lam, M.J. Kurth, Selectively targeting T- and B-cell lymphomas: a benzothiazole antagonist of α4β1 integrin, J. Med. Chem. 52 (2009) 14–19.
[81] A. Turetsky, E. Kim, R.H. Kohler, M.A. Miller, R. Weissleder, Single cell imaging of Bruton's tyrosine kinase using an irreversible inhibitor, Sci. Rep. 4 (2014).
[82] X. Lin, H. Zhu, Z. Luo, Y. Hong, H. Zhang, X. Liu, H. Ding, H. Tian, Z. Yang, Near-infrared fluorescence imaging of non-Hodgkin's lymphoma CD20 expression using Cy7-conjugated obinutuzumab, Mol. Imaging Biol. 16 (2014) 877–887.
[83] B. Holzmann, U. Gosslar, M. Bittner, Alpha 4 integrins and tumor metastasis, in: Leukocyte Integrins in the Immune System and Malignant Disease, vol. 231, 1998, pp. 125–141.
[84] P.J. Neeson, P.J. Thurlow, G.P. Jamieson, C. Bradley, Lymphocyte-facilitated tumour cell adhesion to endothelial cells: the role of high affinity leucocyte integrins, Pathology 35 (2003) 50–55.
[85] R.D. Carpenter, M. Andrei, O.H. Aina, E.Y. Lau, F.C. Lightstone, R. Liu, K.S. Lam, M.J. Kurth, Selectively targeting T- and B-cell lymphomas: a benzothiazole antagonist of alpha(4)beta(1) integrin, J. Med. Chem. 52 (2009) 14–19.
[86] A.J. Mohamed, L. Yu, C.-M. Backesjo, L. Vargas, R. Faryal, A. Aints, B. Christensson, A. Berglof, M. Vihinen, B.F. Nore, C.I.E. Smith, Bruton's tyrosine kinase (Btk): function, regulation, and transformation with special emphasis on the PH domain, Immunol. Rev. 228 (2009) 58–73.
[87] Y.-T. Tai, K.C. Anderson, Bruton's tyrosine kinase: oncotarget in myeloma, Oncotarget 3 (2012) 913–914.
[88] T. Liu, L.Y. Wu, M.R. Hopkins, J.K. Choi, C.E. Berkman, A targeted low molecular weight near-infrared fluorescent probe for prostate cancer, Bioorg. Med. Chem. Lett. 20 (2010) 7124–7126.
[89] X. Yi, F. Yan, F. Wang, W. Qin, G. Wu, X. Yang, C. Shao, L.W.K. Chung, J. Yuan, IR-780 dye for near-infrared fluorescence imaging in prostate cancer, Med. Sci. Monit. 21 (2015) 511–517.
[90] Y. Chen, S. Dhara, S.R. Banerjee, Y. Byun, M. Pullambhatla, R.C. Mease, M.G. Pomper, A low molecular weight PSMA-based fluorescent imaging agent for cancer, Biochem. Biophys. Res. Commun. 390 (2009) 624–629.
[91] B.P. Neuman, J.B. Eifler, M. Castanares, W.H. Chowdhury, Y. Chen, R.C. Mease, R. Ma, A. Mukherjee, S.E. Lupold, M.G. Pomper, R. Rodriguez, Real-time, near-infrared fluorescence imaging with an optimized dye/light source/camera

ITM Exhibit 1023, Page 15 of 16

combination for surgical guidance of prostate cancer, Clin. Cancer Res. 21 (2015) 771–780.
[92] J. Yuan, X. Yi, F. Yan, F. Wang, W. Qin, G. Wu, X. Yang, C. Shao, L.W.K. Chung, Near-infrared fluorescence imaging of prostate cancer using heptamethine carbocyanine dyes, Mol. Med. Rep. 11 (2015) 821–828.
[93] X. Yang, C. Shi, R. Tong, W. Qian, H.E. Zhau, R. Wang, G. Zhu, J. Cheng, V.W. Yang, T. Cheng, M. Henary, L. Strekowski, L.W.K. Chung, Near IR heptamethine cyanine dye-mediated cancer imaging, Clin. Cancer Res. 16 (2010) 2833–2844.
[94] X. Wang, S.S. Huang, W.D.W. Heston, H. Guo, B.-C. Wang, J.P. Basilion, Development of targeted near-infrared imaging agents for prostate cancer, Mol. Cancer Ther. 13 (2014) 2595–2606.
[95] S. Jeschke, L. Lusuardi, A. Myatt, S. Hruby, C. Pirich, G. Janetschek, Visualisation of the lymph node pathway in real time by laparoscopic radioisotope- and fluorescence-guided sentinel lymph node dissection in prostate cancer staging, Urology 80 (2012) 1080–1086.
[96] Y. Wang, T. Liu, E. Zhang, S. Luo, X. Tan, C. Shi, Preferential accumulation of the near infrared heptamethine dye IR-780 in the mitochondria of drug-resistant lung cancer cells, Biomaterials 35 (2014) 4116–4124.
[97] A. Becker, B. Riefke, B. Ebert, U. Sukowski, H. Rinneberg, W. Semmler, K. Licha, Macromolecular contrast agents for optical imaging of tumors: comparison of indotricarbocyanine-labeled human serum albumin and transferrin, Photochem. Photobiol. 72 (2000) 234–241.
[98] Z.-H. Jin, V. Josserand, S. Foillard, D. Boturyn, P. Dumy, M.-C. Favrot, J.-L. Coll, In vivo optical imaging of integrin alpha(v)-beta(3) in mice using multivalent or monovalent cRGD targeting vectors, Mol. Cancer 6 (2007).
[99] M. Dasari, S. Lee, J. Sy, D. Kim, S. Lee, M. Brown, M. Davis, N. Murthy, Hoechst-IR: an imaging agent that detects necrotic tissue in vivo by binding extracellular DNA, Org. Lett. 12 (2010) 3300–3303.
[100] R.S. Agnes, A.-M. Broome, J. Wang, A. Verma, K. Lavik, J.P. Basilion, An optical Probe for noninvasive molecular imaging of orthotopic brain tumors overexpressing epidermal growth factor receptor, Mol. Cancer Ther. 11 (2012) 2202–2211.
[101] Y. Huang, F. Hu, R. Zhao, G. Zhang, H. Yang, D. Zhang, Tetraphenylethylene conjugated with a specific peptide as a fluorescence turn-on bioprobe for the highly specific detection and tracing of tumor markers in live cancer cells, Chem. A Eur. J. 20 (2014) 158–164.
[102] E. Kim, K.S. Yang, R.H. Kohler, J.M. Dubach, H. Mikula, R. Weissleder, Optimized Near-IR Fluorescent Agents for in Vivo Imaging of Btk Expression, Bioconjugate Chem. 26 (8) (2015) 1513–1518.
[103] F. Lv, X. He, L. Wu, T. Liu, Lactose substituted zinc phthalocyanine: a near infrared fluorescence imaging probe for liver cancer targeting, Bioorg. Med. Chem. Lett. 23 (2013) 1878–1882.
[104] T. Ishizawa, N. Fukushima, J. Shibahara, K. Masuda, S. Tamura, T. Aoki, K. Hasegawa, Y. Beck, M. Fukayama, N. Kokudo, Real-time identification of liver cancers by using indocyanine green fluorescent imaging, Cancer 115 (2009) 2491–2504.
[105] T. Nakajima, K. Sano, M. Mitsunaga, P.L. Choyke, H. Kobayashi, Real-time monitoring of in vivo acute necrotic cancer cell death induced by near infrared photoimmunotherapy using fluorescence lifetime imaging, Cancer Res. 72 (2012) 4622–4628.
[106] H. Ra, E. Gonzaez-Gonzaez, M.J. Uddin, B.L. King, A. Lee, I. Ali-Khan, L.J. Marnett, J.Y. Tang, C.H. Contag, Detection of non-melanoma skin cancer by in vivo fluorescence imaging with fluorocoxib A, Neoplasia 17 (2015) 201–207.
[107] A. Becker, C. Hessenius, K. Licha, B. Ebert, U. Sukowski, W. Semmler, B. Wiedenmann, C. Grotzinger, Receptor-targeted optical imaging of tumors with near-infrared fluorescent ligands, Nat. Biotechnol. 19 (2001) 327–331.
[108] N.K. Tafreshi, X. Huang, V.E. Moberg, N.M. Barkey, V.K. Sondak, H. Tian, D.L. Morse, J. Vagner, Synthesis and characterization of a melanoma-targeted fluorescence imaging probe by conjugation of a melanocortin 1 receptor (MC1R) specific ligand, Bioconjugate Chem. 23 (2012) 2451–2459.
[109] N.K. Tafreshi, A. Silva, V.C. Estrella, T.W. McCardle, T. Chen, Y. Jeune-Smith, M.C. Lloyd, S.A. Enkemann, K.S.M. Smalley, V.K. Sondak, J. Vagner, D.L. Morse, In vivo and in silico pharmacokinetics and biodistribution of a melanocortin receptor 1 targeted agent in preclinical models of melanoma, Mol. Pharm. 10 (2013) 3175–3185.
[110] T. Miyamoto, N. Tanaka, Y. Eishi, T. Amagasa, Transferrin receptor in oral tumors, Int. J. Oral Maxillofac. Surg. 23 (1994) 430–433.
[111] A. Rudkouskaya, S. Rajoria, L. Zhao, X. Intes, M.M. Barroso, Fluorescence lifetime FRET measures transferrin tumor uptake using in vivo small animal imaging: Implications in the development of targeted drug therapy for estrogen receptor positive breast cancer, Mol. Biol. Cell 25 (2014).
[112] S. Dixit, T. Novak, K. Miller, Y. Zhu, M.E. Kenney, A.-M. Broome, Transferrin receptor-targeted theranostic gold nanoparticles for photosensitizer delivery in brain tumors, Nanoscale 7 (2015) 1782–1790.
[113] X.-Q. Jiang, S.-M. Guo, M. Zhang, M. Zhou, B.-C. Ye, DNA-hosted Hoechst dyes: application for label-free fluorescent monitoring of endonuclease activity and inhibition, Analyst 139 (2014) 5682–5685.
[114] B. Willis, D.P. Arya, Recognition of RNA duplex by a neomycin-Hoechst 33258 conjugate, Bioorg. Med. Chem. 22 (2014) 2327–2332.
[115] C. Mo, Y. Lu, Y. Deng, J. Wang, L. Xie, T. Li, Y. He, Q. Peng, X. Qin, S. Li, LAPTM4B polymorphism increases susceptibility to multiple cancers in Chinese populations: a meta-analysis, BMC Genet. 15 (2014).
[116] M. Xiao, S. Jia, H. Wang, J. Wang, Y. Huang, Z. Li, Overexpression of LAPTM4B: an independent prognostic marker in breast cancer, J. Cancer Res. Clin. Oncol. 139 (2013) 661–667.
[117] K. Ndiaye, P.D. Carriere, J. Sirois, D.W. Silversides, J.G. Lussier, Differential expression of lysosome-associated protein transmembrane-4 beta (LAPTM4B) in granulosa cells of ovarian follicles and in other bovine tissues, J. Ovar. Res. 8 (2015).
[118] H. Zhang, S. Qi, T. Zhang, A. Wang, R. Liu, J. Guo, Y. Wang, Y. Xu, miR-188-5p inhibits tumour growth and metastasis in prostate cancer by repressing LAPTM4B expression, Oncotarget 6 (2015) 6092–6104.
[119] S.-P. Wang, S. Iwata, S. Nakayamada, H. Niiro, S. Jabbarzadeh-Tabrizi, M. Kondo, S. Kubo, M. Yoshikawa, Y. Tanaka, Amplification of IL-21 signalling pathway through Bruton's tyrosine kinase in human B cell activation, Rheumatology 54 (2015) 1488–1497.
[120] M. Ito, T. Shichita, M. Okada, R. Komine, Y. Noguchi, A. Yoshimura, R. Morita, Bruton's tyrosine kinase is essential for NLRP3 inflammasome activation and contributes to ischaemic brain injury, Nat. Commun. 6 (2015).
[121] L. Alinari, C. Quinion, K.A. Blum, Bruton's tyrosine kinase inhibitors in B-cell non-Hodgkin's lymphomas, Clin. Pharmacol. Ther. 97 (2015) 469–477.
[122] Y. Wang, L.L. Zhang, R.E. Champlin, M.L. Wang, Targeting Bruton's tyrosine kinase with ibrutinib in B-cell malignancies, Clin. Pharmacol. Ther. 97 (2015) 455–468.
[123] D.J. Peng, J. Sun, Y.Z. Wang, J. Tian, Y.H. Zhang, M.H.M. Noteborn, S. Qu, Inhibition of hepatocarcinoma by systemic delivery of Apoptin gene via the hepatic asialoglycoprotein receptor, Cancer Gene Ther. 14 (2007) 66–73.
[124] H. Sato, Y. Kato, E. Hayashi, T. Tabata, M. Suzuki, Y. Takahara, Y. Sugiyama, A novel hepatic-targeting system for therapeutic cytokines that delivers to the hepatic asialoglycoprotein receptor, but avoids receptor-mediated endocytosis, Pharm. Res. 19 (2002) 1736–1744.
[125] G. Ashwell, J. Harford, Carbohydrate-specific receptors of the liver, Annu. Rev. Biochem. 51 (1982) 531–554.
[126] Z. Koltai, P. Vajdovich, V. Dekay, Cyclooxygenase-2 (COX-2) expression in domestic animal tumours. Literature review, Magy. Allatorvosok Lapja 136 (2014) 579–587.
[127] O. Tietz, A. Marshall, M. Wuest, M. Wang, F. Wuest, Radiotracers for molecular imaging of cyclooxygenase-2 (COX-2) enzyme, Curr. Med. Chem. 20 (2013) 4350–4369.
[128] B. Ogretmen, Y.A. Hannun, Biologically active sphingolipids in cancer pathogenesis and treatment, Nat. Rev. Cancer 4 (2004) 604–616.
[129] S. Combemale, C. Santos, F. Rodriguez, V. Garcia, C. Galaup, C. Frongia, V. Lobjois, T. Levade, C. Baudoin-Dehoux, S. Ballereau, Y. Genisson, A biologically relevant ceramide fluorescent probe to assess the binding of potential ligands to the CERT transfer protein, RSC Adv. 3 (2013) 18970–18984.

ITM Exhibit 1023, Page 16 of 16